



iJRASET

International Journal For Research in
Applied Science and Engineering Technology



INTERNATIONAL JOURNAL FOR RESEARCH

IN APPLIED SCIENCE & ENGINEERING TECHNOLOGY

Volume: 12 Issue: IV Month of publication: April 2024

DOI: <https://doi.org/10.22214/ijraset.2024.59592>

www.ijraset.com

Call:  08813907089

E-mail ID: ijraset@gmail.com

Breast Cancer Tumour Masks Segmentation Using Modified U-Net with Channel Attention

Akin-Olayemi Titilope.Helen¹, Ojo Abayomi Fagbuagun², Oguntuase R. Abimbola³, Ojo Olufemi A⁴, Makinde Bukola Oyeladun⁵

¹Department of Computer Science, Federal Polytechnic Ado-Ekiti, Ado-Ekiti, Ekiti State Nigeria

²Department of Computer Science, Federal University, Oye-Ekiti

³Department of Computer Science, Federal Polytechnic Ado-Ekiti, Ado-Ekiti, Ekiti State.Nigeria

⁴Department of Computer Science, Federal Polytechnic Ado-Ekiti, Ado-Ekiti, Ekiti State Nigeria

⁵Department of Computer Science, Osun State College of Technology, Esa-Oke Nigeria

Abstract: A modified U-Net for biomedical image segmentation with channel attention is developed for breast cancer image segmentation. A unique step in biomedical image analysis is segmentation because it determines the accuracy of image analysis algorithms. Algorithms for accurate and early breast cancer detection in women using mammograms depend highly on the accuracy of the segmentation stage. In this thesis, in order to improve on the segmentation ability of the traditional U-Net architecture, it was modified by varying the fixed kernel sizes that it was originally designed for. In this model, progressively increasing kernel sizes of 3x3, 5x5, 7x7, 9x9 and 11x11 were used, which is different from the architecture of U-Net that depended on fixed 3x3 kernel sizes for all convolutional layers. The first Convolutional block of the proposed model contains two Conv2D layers with 3x3 kernel sizes, ReLU (Rectified Linear Unit) activation function, and 16 channel dimensions. A maxpooling2D layer with pool size of (2x2) was placed to downsample the image size before feeding to the next convolutional block which used the same activation function, with 32 channel dimension and 5x5 kernel size. The next convolutional block used 64 channel dimensions with 7x7 kernel size, then a 9x9 kernel size Conv2D block with 128 channel dimensions was placed before the Conv2D with upsampling. The squeeze and excitation block was placed after this convolutional layer and in-between the two convolutional blocks with 11x11 kernel sizes, to reallocate the weight of the essential features to ensure that more discriminate features are learnt from the breast cancer images to improve the overall representational strength of the network through the performance of dynamic feature recalibration of the image channels. This significantly improved the performance of the segmentation by explicitly modeling the interdependencies between channels in the convolutional layers. The increasing kernel sizes enables the model to learn more discriminate features from the images. Jaccard similarity index, F1 score, Recall, Precision, F2 score, and accuracy results were used to compare the result of the proposed model with other models such as U-Net model and Baseline model. The results shows a better performance of 0.88 for Jaccard similarity index, 0.94 for F1 score, 0.93 for recall, 0.92 for precision, 0.92 for F2 score, and an accuracy score of 0.98%. The model is good for biomedical image segmentation.

Keywords: Biomedical, Segmentation, Breast Cancer, Biometric, Convolutional, Kernels

I. INTRODUCTION

When division of cells in the breasts goes out of control, it leads to breast cancer. Breast cancer is widely known, and research has shown that one out of eight women will possibly be diagnosed with cancer of the breast through their life span, and over 40,000 women die of cancer of the breast yearly (National Breast Cancer Foundation (NBCF), 2016). Early research on breast cancer, according to Moody *et al.*, (2005), proved that metastization, which means cancer's spread from the breast to other body parts mainly causes death in many women. Breast cancer diagnosis could be done by tumor classification. Tumour classification could be achieved in four (4) ways; which are Mammography, biopsy, self-examination of the breast, and near infrared fluorescence (NIF). However, mammography and biopsy are the generally accepted ways through which classification can be done (Khan, *et al.*, 2019). In mammography, the images of the breast are used by the radiologist to detect early symptoms of cancer in women..

While in the biopsy, a pathologist analyzes tissue samples from an affected breast region under the microscope to detect and classify the tumor. Breast tumors can be of two lesions (benign and malignant).

The non-cancerous tumors are being classified as benign lesion while the malignant lesions are cancerous tumors. Mammography is the most accepted way of diagnosing cancer because of the complex nature of biopsy (Chekkoury *et al.*, 2012). The world health organization emphasized that the early diagnosis of breast cancer leads to an increase in the survival rate in women to over 80% (WHO, 2014). To ensure that breast cancer is diagnosed early, various methods of detection have been proposed by the radiologists. However, the development in artificial intelligence has seen different computer scientists contribute their quota through the deep and machine learning techniques. Nevertheless, the problems of low accuracy that is being attributed to insufficient datasets and defective data pre-processing still linger.

Recently, the challenges of insufficient datasets have been minimized through adopting various data augmentation and data generation techniques. An example of such methods is the use of variable auto-encoders (Doersch, 2016), and also Generative Adversarial Networks (GANs) (Goodfellow, 2016), to generate synthetic images. For easy diagnosis and treatment, it is crucial to segment biomedical images. Segmentation involves delineating tumor areas from the whole image. However, problems of effectively segmenting tumors from breast cancer images for easy diagnosis and treatment have not been fully addressed. Also, the existing segmentation models often come with high complexity based on the size of such models. This challenge is often attributed to the varying shapes and sizes of the tumors in breast cancer. This research aims to improve the success segmentation rate of tumors from breast cancer images by developing a biomedical segmentation model that is capable of detecting breast cancer tumors from breast images with improved performance, while minimizing model complexity.

Research reveals the early detection of breast cancer tumors often reduces the mortality rate since it will allow the medical expert to commence appropriate treatment as soon as it is detected. Generally, a breast cancer diagnosis is carried out through Mammography, self-examination of the breast, Biopsy or NIF. Nevertheless, biopsy and the use of mammograms are the general way of diagnosing breast cancer (Khan, *et al.*, 2019). The limitations of the biopsy method is its complexity because the amount of tissue obtained from a biopsy needle may not be sufficient due to the fact that the examination is limited to the affected region of the breast as discussed in the previous section. This has made mammography the generally accepted method of diagnosis. Mammography involves checking the scanned images of the breast to detect the presence of malignant or benign cancers.

Generally, an expert is needed to check the mammograms to detect the presence of cancers manually. However, this method is not so reliable since the interpretation of mammograms is subject to variability due to individual interpretations. Moreover, manual detection is time-consuming, expensive, and reliant on the expert's abilities and competence. Also, malignant cancers are challenging to identify. Because of this, recent advancements in artificial intelligence have been proposed as the solution to tackling issues relating to manual diagnosis.

In literature, many deep learning models and machine learning techniques have been proposed in order to achieve better breast cancer diagnosis. Several researchers have presented different machine learning methods for automated cell classifications in breast cancer detection throughout the last few decades. Some researchers have focused on mammogram analysis, collecting traits from mammograms that could be useful for classification of cancer into either malignant or benign cells. However, the complexity of data preprocessing, extraction of features, and classification techniques have not allowed machine learning methods to achieve very precise and state-of-the-art detection and segmentation accuracy. Because of this, deep learning methods have been adopted. (Khan, *et al.*, 2019). Many layers of image representation can be learned by deep learning models to model complicated nonlinear connections in data, allowing them to find more abstract, and valuable characteristics that made it simpler to get relevant information for high-level decision making tasks like classification, segmentation, and prediction. Methods of deep learning require a high number of labelled training images to be optimally trained due to the enormous list of parameters that are usually involved.

In breast cancer images, malignant tumors often come in various shapes and sizes. Therefore, it is paramount to segment these tumours for easy diagnosis and treatment to prevent mortality. A unique step in image analysis is image segmentation and it affects accuracy of image analysis (Michael *et al.*, 2021). This means that the result of segmentation is presented to later stages of image analysis. Once this stage is not accurate, it affects the remaining stages of the image analysis. However, existing segmentation models developed for breast cancer segmentation have also been unable to achieve state-of-the-art result due to these

tumours' varying shapes and sizes. Likewise, the existing models often come with bulky model sizes, and researchers have investigated how to realize state-of-the-art segmentation results without incurring additional model parameters.

Several researchers have proposed various techniques for achieving higher accuracy in early breast cancer detection and segmentation from cancer images. Researchers such as Usha, (2010), Boquete *et al.*, (2012) Cardoso *et al.*, (2016), (Khan *et al.*, 2019), among others have proposed deep learning techniques.

However, limitations of low segmentation performance and bulky model segmentation model size are the motivation for this research.

II. THEORETICAL BACKGROUND

A. Breast Cancer

The female breast, also called mammary gland, it is situated on the anterior section of the chest wall. It is made up of glandular tissue having a very dense, and fibrous stromal. There are multiple ducts in the breast which connect the lobular units that secrete milk to the nipple of the breast. The milk is as a very significant source of food for babies (America Joint Committee on Cancer (AJCC), 2002). The necessities of breastfeeding to babies cannot be overemphasized. However, the breast can be affected by various infections and the most common infection, among which the commonest is breast cancer, which is significant source of health challenge that affects women, which cut across all ages, and races. Cancer of the breast occurs when breast tissues are infected.

According to medical doctors, cancer of the breast occurs due to uncontrollable cell division in the breast. These cells develop faster than healthy cells and keep growing without control, resulting in lump or mass. Cancer cells in breast have the tendency to spread or metastasize to lymph nodes and other body parts. As shown in Figure 2.1, the most common source of breast cancer is attributed to cells in breast that produce milk being invaded, which is known as ductal carcinoma. Cancer of the breast begins in lobules which are glandular tissues. It can also begin from other cell in the breast. The increase in risk of cancer of the breast can be linked with hormonal, lifestyle, and environmental variables based on research (Rouhi *et al.*, 2015).

Early symptoms of breast might include a sudden change in the shape of the breast, swollen lymph node, breast lump, dimpling of the breast skin, and discharge of fluid from the nipple; among others. Fluid discharge is the commonest form of cancer that affects women globally, and it has resulted in roughly 570,000 death cases since the year 2015. Furthermore, more than 1.5 million women, accounting for 25% of all women suffering from cancer, are diagnosed of cancer of the breast worldwide. (Stewart & Wild, 2014).

Cancer of the breast occurs in steps and it involves many type of cells. Due to this phenomenon, the prevention of cancer of the breast is still a huge challenge for scientists worldwide. The metastatic ability of cancer of the breast enables it to migrate to other body organs which may include the bone, lung, brain, and the liver, among other body parts. This is responsible for the incurable nature of cancer (Moody *et al.*, 2005). Although the incidence of global breast cancer increases on yearly basis, but the rate of mortality decreases because of early screening of the disease (Sun *et al.*, 2017).

As stated earlier, breast cancer can be detected from the presence of lumps, micro-calcifications, and asymmetry regions of the breast. It can also be detected by the presence of distortion in the breast. The presence of masses are the most characteristic and prevalent sort of abnormality among them. On the other hand, masses can be disguised by overlaying tissues of the breast, and this makes the detection of breast cancer difficult. Furthermore, specific breast tissues morphologically resemble masses and are therefore mistaken as masses (Awad *et al.*, 2020).

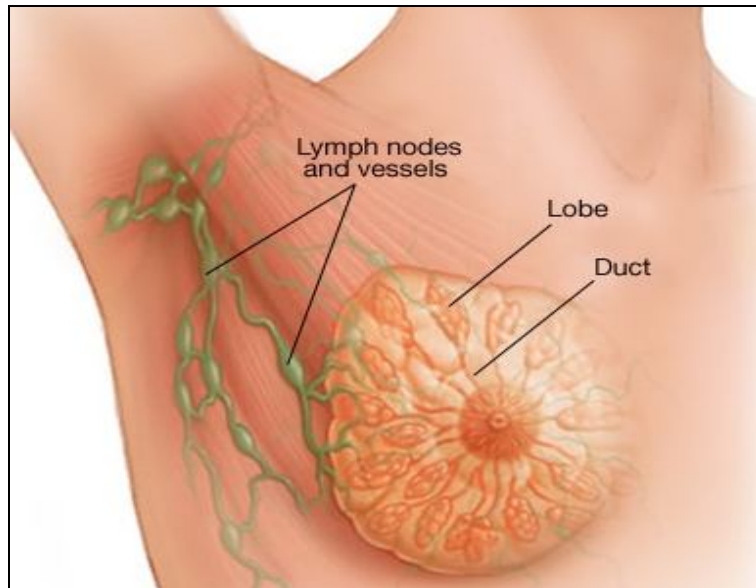


Figure 2. 1: Target Areas in the Breast

Generally, cancer tissues with greater pixel intensities can be recognised more quickly than the rest of the breast. Breasts that are dense have intensities similar to those seen in cancerous areas, and tumour areas must be correctly detected (Zheng et al., 2020). According to Vargas et al (2003), early detection of cancer of the breast tend to increase the rate of survival of people suffering from cancer of the breast. This is because quick treatments prevent it from being metastatic. In order to reduce the mortality rate, early treatment regime must be readily available and accessible after early detection of the disease (Vargas et al., 2003). In figure 2.2, the formation of cancer of the breast is illustrated.

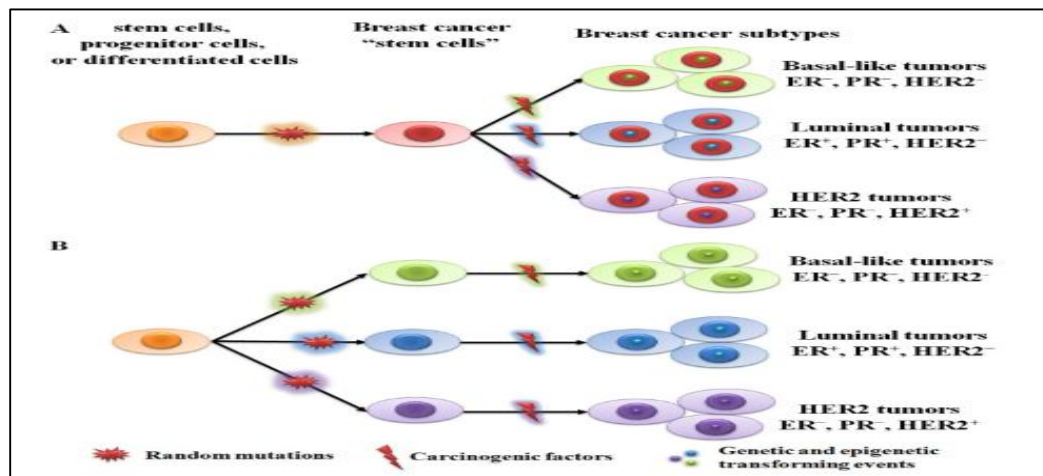


Figure2. 2: The hypothetical theories of breast cancer initiation and progression

[Source: (Sun *et al.*, 2017)]

where ER represent Estrogen, PR represent Progesterone, and HER2 represents Human epidermal growth factor receptor Researchers have tried to detect the primary cause of breast cancer. The next section describes some reasons that have been highlighted in the literature.

- 1) Age: In the year 2016, almost 99.3% and 71.2% of all breast cancer-related global deaths were reported in women that are over age 40, and 60 (Siegel et al., 2017). Based on this research, it could be recommended that women who are above this age should have mammography screenings at intervals

- 2) **Reproduction Factors:** Reproduction factors which may include early menarche, delayed menopause, late age occurring at first pregnancy, and low parity tend to increase the risk of breast cancer. Research in Horn and Vatten, (2017) stated that a 1-year delay in menarche, or each additional birth, decreases the risk of breast cancer by about 5% or 10%, respectively.
- 3) **Modern Lifestyle:** Modern lifestyles like taking excessive alcohol and excessive dietary fat intake, can lead to an increase in the risk of breast cancer. Consumption of alcohol can raise the level of oestrogen-related hormones in the blood, and activate oestrogen receptor (Dall and Britt, 2017). A schematic diagram showing the causes of cancer of the breast in women is depicted in Figure 2.3.

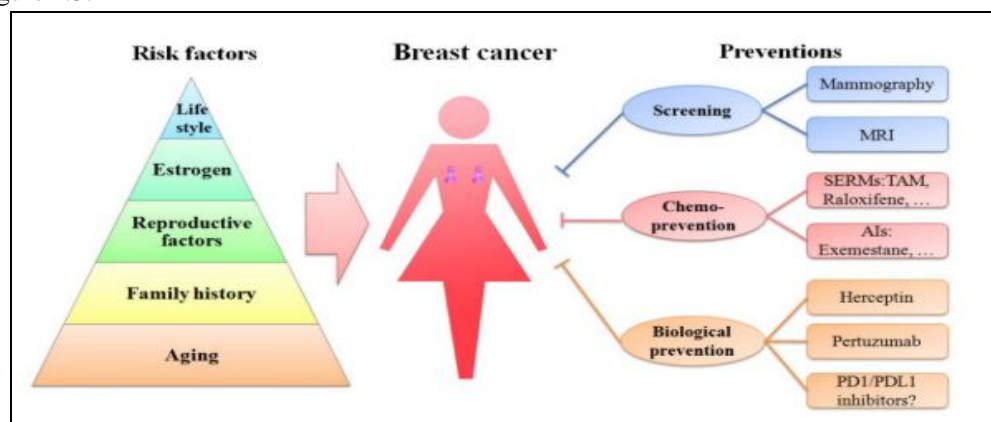


Figure 2. 3: Schematic diagram of the risk factors of breast cancer in women

Breast cancer disease can be prevented, the developed countries made available the adequate medical resources which can protect against this disease, such as the daily use of chemo preventative medications or annual mammography screening (Lynch, et al., 2011). However, the essential preventive factor is early breast cancer detection. The detection of breast cancer at the early stage has proved to improve the survival rate of patients. Figure 2.4 shows the survival rate percentage per stage of breast cancer (Zheng et al., 2020).

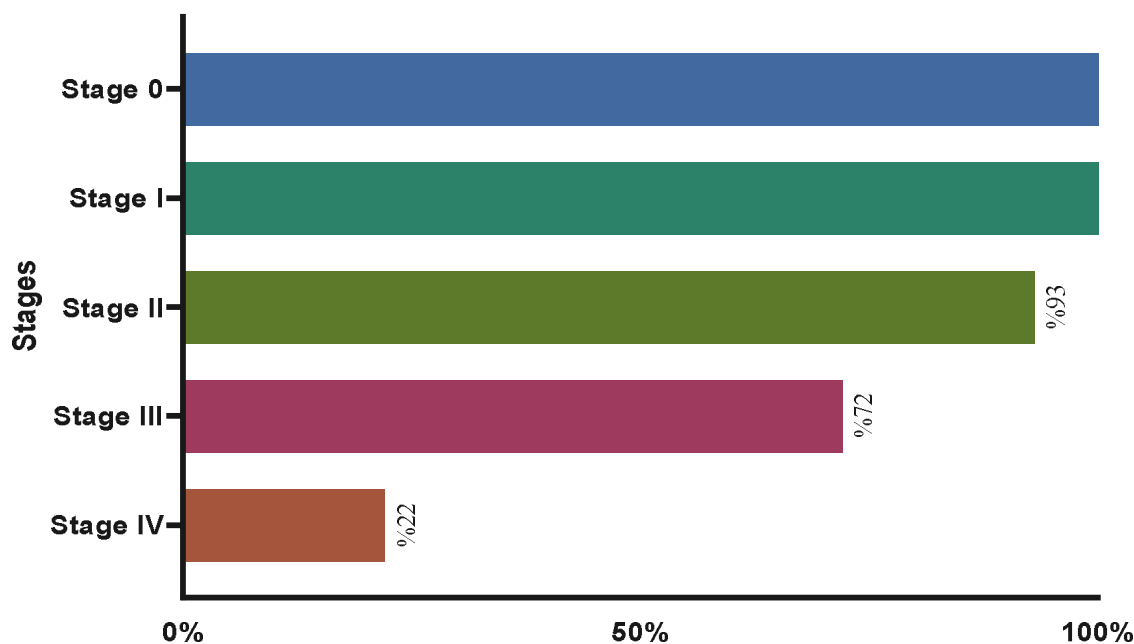


Figure 2. 4: Survival rate percentage per stage

To detect breast cancer, two major approaches are adopted; mammography and biopsy (Khan, et al., 2019). Research conducted has shown that Near Infrared Fluorescence (NIRF) is an essential tool in the diagnosis of breast cancer (Li et al., 2017). However,

the self-check approach is the most common, also called Self Breast Examination (SBE). As shown in Figure 2.5, SBE involves the woman pressing and checking the breast to detect the presence of lumps or irregular discharge. This technique is often unreliable, as the lumps must have grown to a particular size before they can be felt through SBE. Therefore, this technique is not recommended in the context of early detection. The sizes of lumps discoverable through SBE are depicted in Figure 2.6.

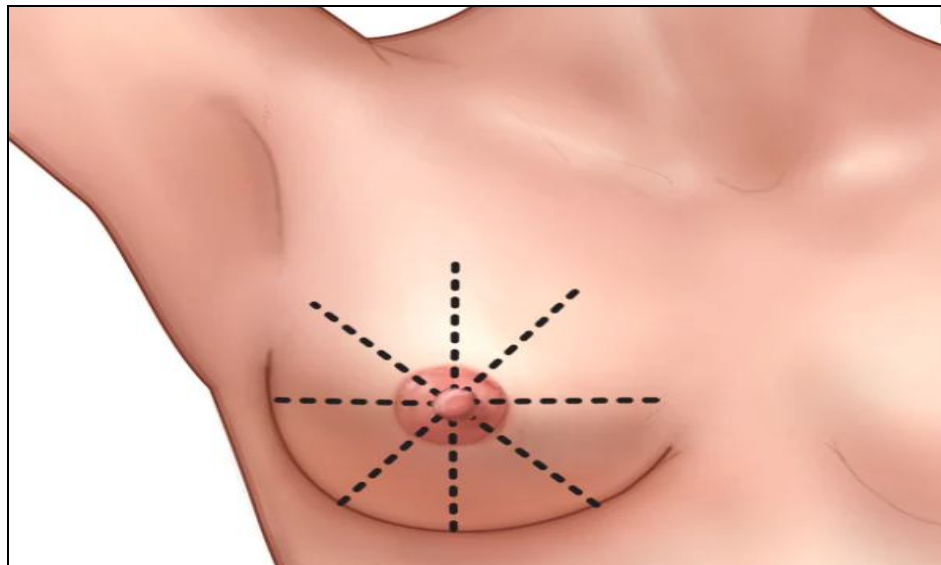


Figure 2. 5: Self breast examination

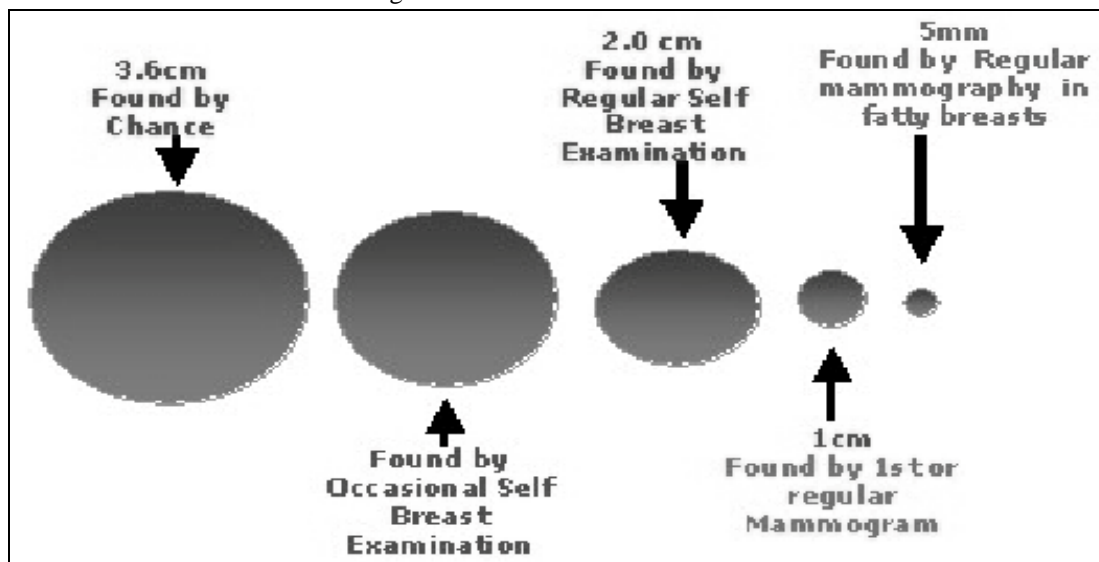


Figure 2. 6: Lump sizes discoverable by Self Breast Examination (SBE)

Mammography involves the use of breast images to carry out early detection of cancer symptoms in women. This is usually carried out by a radiologist. In mammography, breast images are used to detect early cancer symptoms in women by the radiologist. While in the biopsy, a sample of tissue from an affected region of the breast is analyzed under a microscope by a pathologist for the purpose of detecting and classification of breast tumor. Two tumor types could be detected in the work of a pathologist, which could be malignant or benign. The benign tumor lesion can be grouped as non-cancerous, while malignant lesion is the cancerous. Due to the complex nature of biopsy, mammography has become the most acceptable approach to breast cancer diagnosis (Chekkoury et al., 2012).

B. Mammography

Mammography involves the use of a special medical imaging instrument that uses low-dose of x-ray system to view the inside of breasts to check for benign or malignant cancers. A mammogram, helps in carrying out early detection, and diagnosis of cancer of the breast in women, and it is carried out by a radiologist. An example of a mammogram is shown in Figure 2.7.

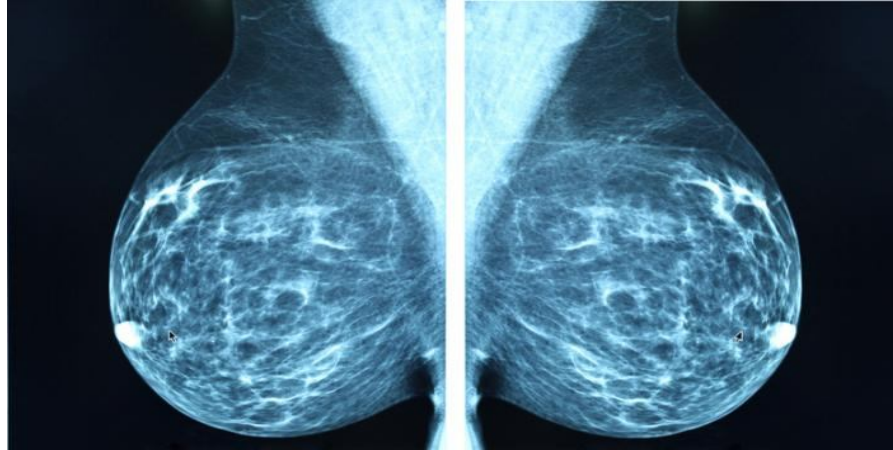


Figure 2. 7: A mammogram

A critical tool that medical doctors have been using for screening and diagnosis of breast cancer is a mammogram. It can also be used for evaluation and follow up on women with cancer disease. Two stages are involved in mammography: in the first stage, the breast is squeezed between two flat plates. In the second stage, the breast is then exposed to mild X-ray dosage, and detected by a two-dimensional panel detector (Awad et al., 2020).

National Cancer Institute (NCI) attempted to classify mammograms into two types namely:

- 1) *Screening mammogram*: This type involves breast X-rays that are used to detect changes in the breast of women without any sign or symptoms of breast cancer. It involved the X-rays of the two breasts. Mammograms helps in the detection of breast tumor which cannot be felt with the hands.
- 2) *Diagnostic Mammogram*: Diagnostic mammogram can be used to diagnose the unusual changes that occur in the breast such as lumps, pains, and discharge from nipples. It can be used in the evaluation of abnormalities which are detected on a screening mammogram.

Mammography can be done in three ways. One of the ways is through digital mammography, the second way is computer-aided detection, while the third is breast tomosynthesis. A digital mammography system is a type of mammography where the x-rays are converted from a film to a digital image. Similar to digital cameras, digital mammography involves the use of electronics to convert the x-rays from a film into a digital image. The efficiency of these systems allows for better pictures with lower radiation doses. The digital images of the breast are sent to a computer, where they can be viewed by a radiologist, and stored for future reference (Rampun et al. 2018). During a digital mammogram, the patient's experience is similar to that of a traditional film (Mambou et al., 2018).

Computer-aided detection (CAD) systems scan digitized images of your breast to look for areas of high density, high mass, or high level of calcification that may be indicative of cancer. CAD system are used to highlight the areas in the images, which prompt the radiologist to carry out an examination of the area. A process where several images of the breast from various angles are captured for the purpose of reconstruction into a three dimensional image set is known as breasts tomosynthesis. It is an advanced form of breast imaging system.

Mammographic screening has some drawbacks which include cost and technical complexity. One of the main criticisms of the mammography technology is that some women may get False-positive results, which can be harmful to women who do not have breast cancer (see Smith, et al., 2003). Benefits and Risks of Mammography: Table 2.1.

Table 2. 1: Comparison of Benefits and Risks of Mammography

S/N	BENEFITS	RISKS
1	Physician's ability in detecting tumors improves through mammography. Early stage cancers is open to treatment options.	There is always a slight chance of cancer from excessive exposure to radiation
2	Screening mammography can detect small abnormal tissue growth that are limited to milk ducts in breasts.	Five per cent to 15 per cent of screening mammograms require more testing, such as additional mammograms or ultrasound
3	X-ray examination does not have remains of radiation in the body of patients after X-ray examination.	The effective radiation dose for mammography varies per procedure
4	There is no side-effects in the diagnostic range for x-ray examination.	It is not advisable during pregnancy

C. BIOPSY

Biopsy of the breast is a procedure that removes a breast sample before it is sent to the laboratory for testing purposes. The biopsy can be done in three ways (fine needle, core needle and stereotactic biopsy). During a fine needle biopsy, breast cancer patients lies on a table while a small needle and syringe are inserted into the breasts lump to extracts a sample (Spanhol et al., 2016). By this procedure, the main difference that exists between liquid-filled cyst and that of a solid lump could be determined. Several needles are inserted in order to collect samples, which are about the size of rice grain in Core needle biopsy.

In stereotactic biopsy, the patient lie with face down on a table that has a hole, which is electrically powered, and could be adjusted. As the patient's breast is put in place between two plates, he surgeon works underneath the table. The surgeon then create a small incision in order to remove samples with a needle. An illustration of needle biopsy is presented in Figure 2.8

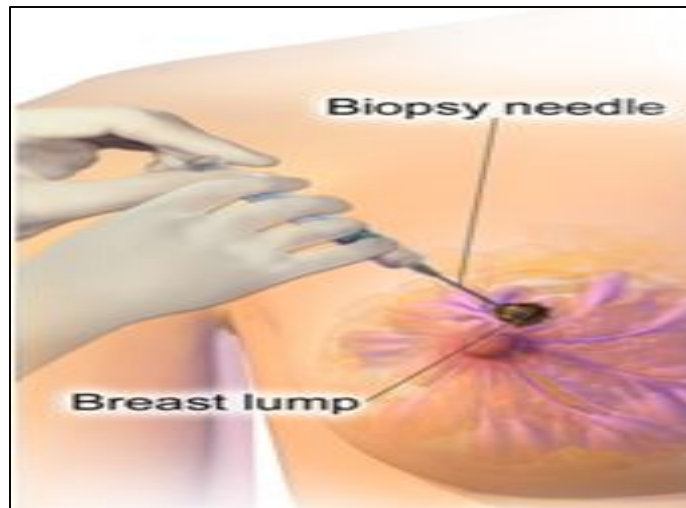


Figure 2. 8: Illustration of biopsy

The major differences that exists between malignant tumour and benign tumour are highlighted in Table 2.2

Table 2.2: Differences between benign and malignant tumours

S/N	Benign tumours	Malignant tumours
-----	----------------	-------------------

1	It doesn't invade nearby tissue	It has the ability to invade nearby tissue
2	It cannot spread to other body parts.	Cells that travel via the human blood or the lymph, or other body parts, can be shed, to form a new tumour.
3	Typically, it doesn't return after removal.	It can return after removal.
4	Possession of regular and smooth shape	The shape is uneven
5	If pushed on, it can move around	They do not move around when pushed on.
6	It does not threaten life	It can threaten life.
7	Treatment may be needed or not.	Treatment is required

Researchers and Radiologists at different levels have proposed various techniques for early detection of cancer of the breast in women because cancer at the early stage are typically more superficial, and cost-effective, than the treatment of advanced cancer (Carlson, et al., 2003). However, the issue remains a significant challenge due to the importance of accurate early detection of the disease (WHO, 2014). Artificial intelligence's advent has allowed computer scientists to contribute to solving this challenge. The following section discusses some researchers who have proposed machine learning technique, and deep learning techniques for early detection of cancer of the breast.

D. Image Analysis Steps

The steps involved in image analysis are image preprocessing, kernel, convolution and max pooling. The following subsection explains the steps.

1) Image Processing

In image processing, images are classified into categories based on image features such as edges, intensity of pixels, and change in image pixel values. In other words, image processing involves the transformation of image into digital form and performing some convolution operations in order to get relevant and useful information from the image. In this process, images are treated as two dimensional signals while performing certain image processing methods such as filtering and convolution.

2) Kernel

Kernel represent the size of a convolution filter that is used to perform convolution on an image. It takes data as an input and then transform it into a required form by performing convolutional filtering operation, extracting features and contributing to the overall segmentation capability of the network.

3) Convolution

This is a mathematical operation that is commonly used in signal processing and image analysis. The term refers to the process of taking two functions and producing a third function, which represents how one function's shape is altered by the shape of the other. In image analysis, convolution involves applying a filter or a kernel to an image. The kernel is a small matrix that slides over the image, performing a mathematical operation at each position.

The operation typically involves multiplying the values of the kernel with corresponding pixel values in the image, and then adding the results to produce a new pixel value in the output image. Convolution is useful in several applications, such as image enhancement, edge detection, smoothing, and feature extraction.

4) Max pooling

This is a pooling operation commonly used in CNN for features extraction in image processing tasks. Its operates by dividing the input image of feature map into non-overlapping rectangular regions, where the maximum value is selected and forwarded to the

next layer, while the other values are discarded. The main purpose is twofold: The spatial down sampling and the Translation invariance.

E. Convolutional Neural Network

Convolutional Neural Network (CNN) can be defined as an end-to-end system where the input to the network is an unprocessed image. The output from a network is a prediction based on distinguishing extracted features from the intermediate layers (Fang et al., 2017). CNN is a sub-class of artificial neural networks which is commonly in finding the solution to complicated problems and it is highly efficient and produce accurate results. (Indolia et al., 2018).

In the convolution layer, we feed the image we want to classify into the nodes of the input layer of the network. The output of the CNN is the predicted class label which is computed from the features that have been extracted from the image, as shown by Fang et al. (2017). There is a connection between the neurons in the present layer and the neurons in the previous layer. The correlation is called the receptive field. The local features can also be extracted from the input image, using the receptive field. For example, if a neuron in our previous layer is associated with a specific region, the receptive field of that neuron will form a weight vector, which stays the same at every point on our plane. The plane refers to our neurons in the following layer. Because the neurons in our plane have equal weights, we can detect similar characteristics at different locations in our input data (see Eghbalian et al. (2018). To create our function map, we slide the weight vector (or filter or kernel) over our input vector.

1) Pooling Layer

Once the position of a feature is located, the feature's exact position becomes less important. Therefore, the pooling (or sub-sampling) layer is preceded by a convolution layer. The major advantage of pooling operation is that the number of training parameters is reduced as well as translational uniformity being introduced. The pooling operation is performed by choosing a window, and then passing the input elements that are within that window via a pooling function, as presented in Fig. 2.9.

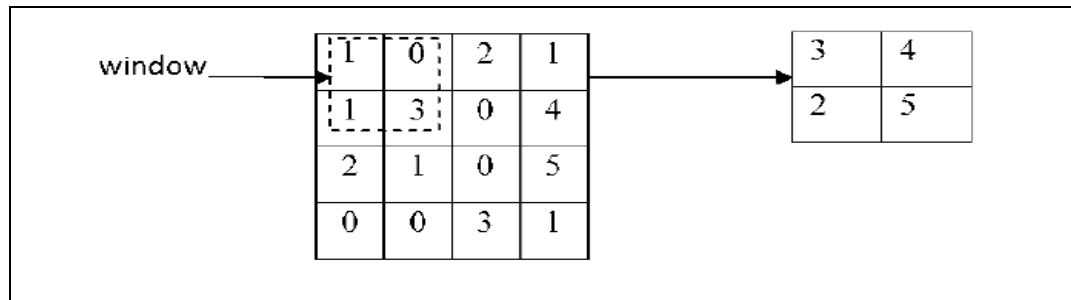


Figure 2. 9: Pooling operation performed by choosing a 2 x 2 window

The pooling function generates another vector. There exist few techniques for pooling operation such as max pooling, and average pooling. In these two techniques the max pooling is the most commonly used that is capable of significantly reducing the map size. When computing errors, the error is not propagated back to winning unit since it does not participate in forward flow (Lee et al., 2017).

2) The fully Connected Layer

The output from the previous phase, and this includes the repeated convolution operations and the pooling, are fed to the fully connected layer of the network. The dot product of the weighted vector is computed. The input vector is also computed for the final output. In order to reduce the cost function through estimation of the cost over a full dataset, a gradient descent learning is implemented. After the first epoch, the parameters are updated, after traversing the entire dataset. This returns global minima. However, a larger training dataset requires a longer training time. This method of getting the cost function reduced is superseded by the stochastic gradient descent. (Liu et al., 2019).

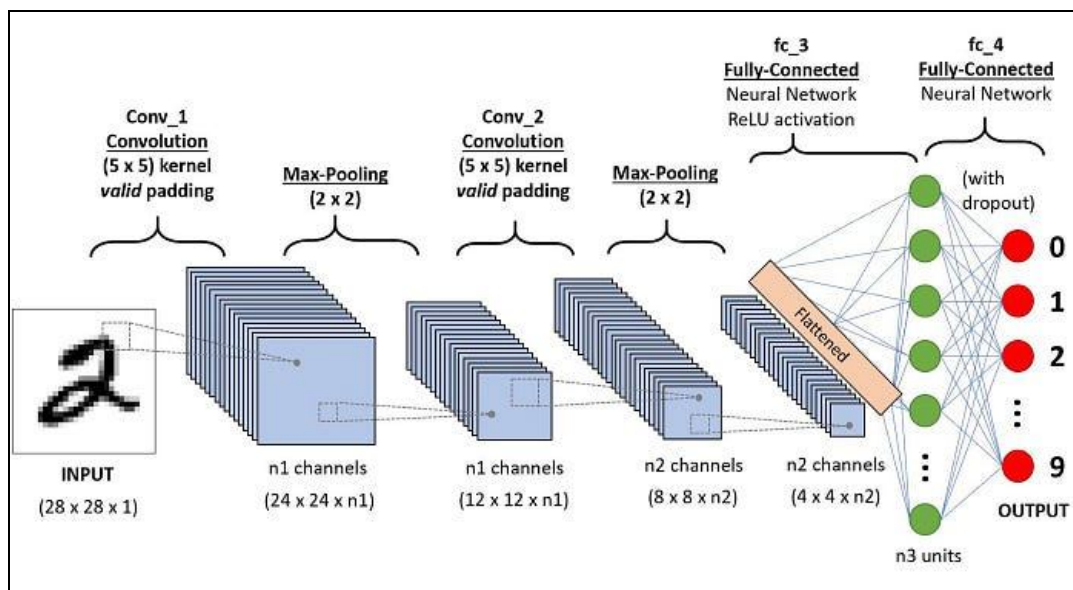


Fig 2.9 Basic architecture of Convolutional Neural Network.

F. Deep Learning In Breast Cancer Detection

Algorithms are available in deep learning that could be used to predict and detect the presence of cancer of the breast in chest radiographs. But the widely used algorithms include Convolutional Neural Networks (CNN), Recurrent Neural Networks (RNN), models that have been pre-trained on large image databases such as googleNet, VGGNet, and ResNet. This is presented in Figure 2.10 Figure 2.12. The common, available, and accessible datasets for model training and testing include the use of mammograms images (Khuriwal, 2018).

Most of these pre-trained models were also based on CNN. A CNN comprises a series of convolutional layers that can extract features from images without requiring feature engineering. As a result, CNN is now the most extensively utilized approach for image interpretation tasks in various disciplines, including the identification and classification of breast cancer.

1) GoogleNet

This also known as inceptionv1, it is a CNN architecture primarily used for image recognition and classification task. It has introduced several innovative features and has the concept of inception modules. These modules uses parallel convolutional layers, with different sizes of filter which gives the network the ability to capture information at different scales and abstraction levels. The architecture have multiple convolution layers, fully connected layers, and pooling layers. It has total of 22 layers. It has been widely used in tasks in computer vision which include classification of images, detection of objects, and semantic segmentation. The architecture of GoogleNet is shown in Fig 2.10.

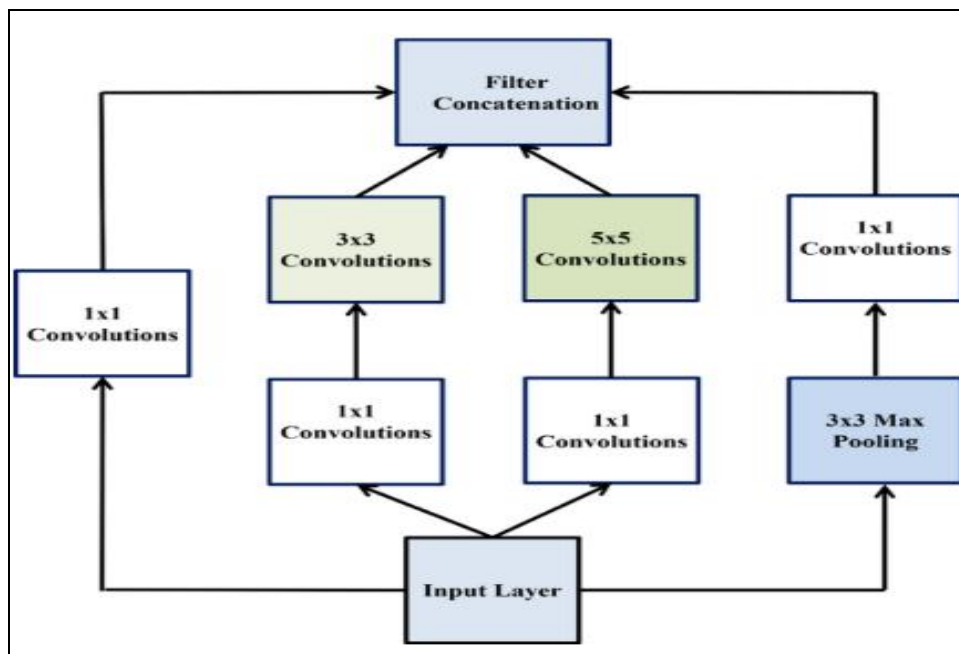


Figure 2. 10: Basic Architecture of GoogleNet

2) ResNet (Residual Network)

ResNet is a model that is based deep learning which can be used for various problem solving purposes in medical image processing and computer vision. Its design is based on the CNN architecture, which is capable of supporting hundreds or even thousands of layers of convolution. The HighwayNet is a hyper-dumb neural network, which is a hyper-deep feedforward neural network. It is the first working hyper-deep neural network that has hundreds of layers.

Skip connections are shortcuts that jump over certain layers. This hyper-dumb network is based on the HighwayNet architecture, which is built on the Hyper-Dumb neural network. It is capable of working hyper-dumb feed forward neural networks, which are hyper-deep neural networks that have hundreds of layers. (Wikipedia 2020)

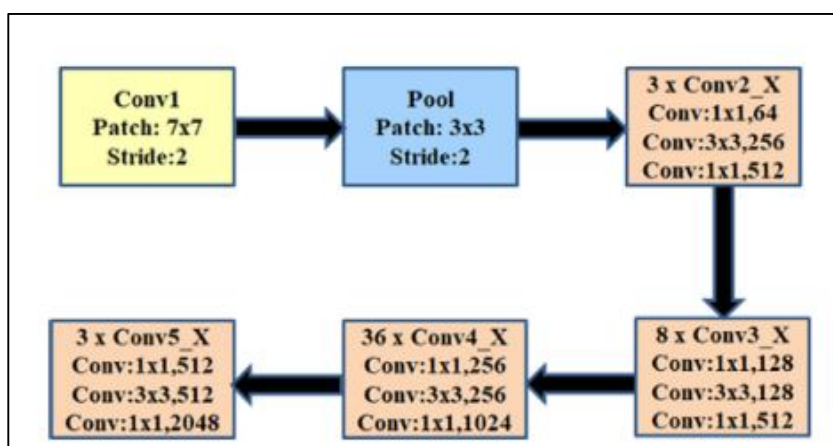


Figure 2. 11: Basic Architecture of ResNet

3) VGGNet (Visual Geometry Group Network)

This network consists of 16 convolution layers, which is very attractive due to its very homogeneous structure. It consists of only 3x3 convolutions with a large number of filters. It has been trained on 4 GPUs over a period of 2 – 3 weeks. Currently, it is the most popular feature extractor in the community. The weight configuration of this network is publicly available. It has been used

as a basic feature extractor in many other apps and challenges. VGGNet, on the other hand, has 138 million parameters. It can be a little difficult to work with. Simonyan and Zisserman (2014).

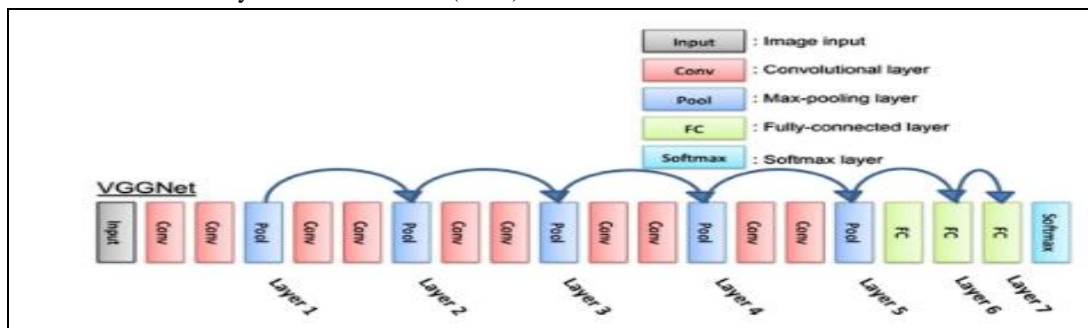


Figure 2. 12: Basic Architecture of VGGNet

Generally, deep learning models can learn from many layers of image data representations in order to acquire the capacity to model complicated non-linear connections in data. This allows deep learning models to find more abstract and valuable characteristics that make extracting relevant features from data for high-level decision tasks such as image segmentation, data classification, and prediction simpler. Deep learning algorithms requires a high number of labelled training data for training due to the enormous number of parameters involved. Deep learning techniques have demonstrated better outstanding prediction outcomes in solutions with huge numbers of training dataset, frequently beating recent classification methods (Cruz-Roa et al., 2017). Several deep learning based models had been proposed in the detection and classification of cancer of the breast, and selections of these models are discussed in the next section.

G. Segmentation Models

According to Ronneberger et al., (2015), the U-net is the most common biomedical image segmentation architecture. It has become a benchmark for other segmentation models. Based on this architecture, many other biomedical image segmentation models have been proposed as it can be seen in Zhou et al., (2018), Yang et al., (2021), among others. Due to the mortality rate of breast cancer, many researchers have focused on developing segmentation models for easy segmentation of tumours in mammograms. For example, Irfan et al., (2021), proposed a dilated semantic segmentation network for medical image segmentation.

Also, channel attention-based module was presented in (H. Lee et al., 2020). The researchers used a multiple scale grid average pooling to carry out semantic image segmentation to ensure that local, and spatial features are learnt to improve segmentation performance. The general mammogram segmentation pipeline was presented in (Michael et al., 2021), shown in Figure 2.13.

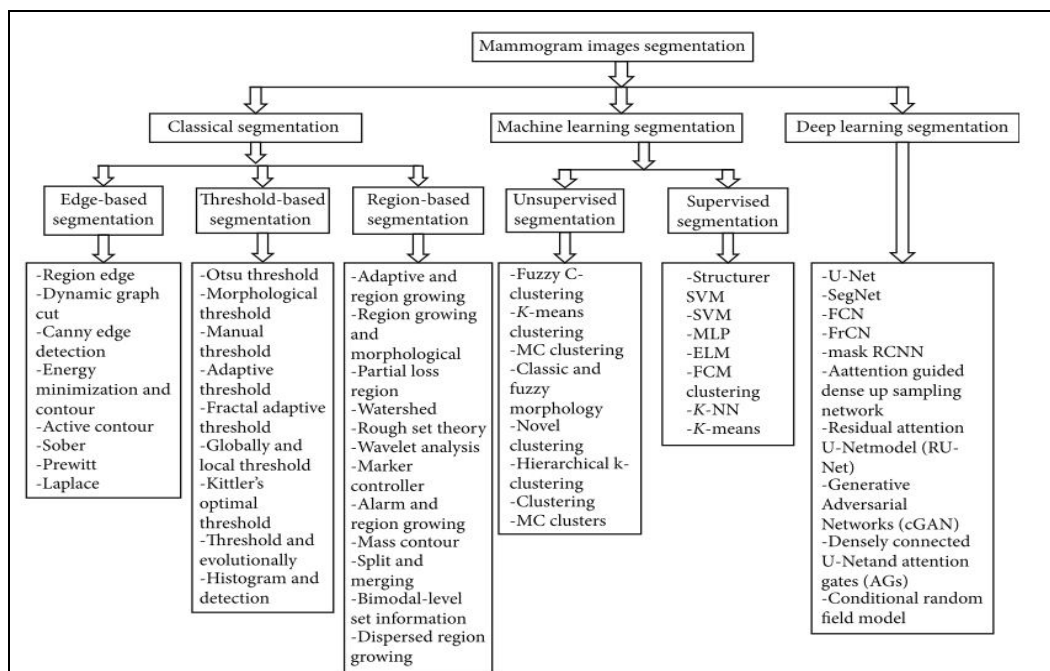


Figure 2.13: Pipeline for mammogram segmentation

As discussed earlier, deep learning techniques have performed well in the detection and segmentation of brain tumours from mammograms. A model that is based on adversarial deep learning network for use in mass segmentation of brain tumour from mammograms was proposed by Zhu et al., (2018). This model is based on a contiguous adversarial FCN-CRF (Fully Convolutional Network with Convolutional Random Fields) network for mammography mass segmentation. Two open datasets, INbreast and DDSM-BCRP (Digital Database for Screening Mammography with Breast Cancer Research Program), were used to test the approach. The proposed strategy attained segmentation rate of 97.0 percent. In Li et al., (2019), the attention-dense U-Net model for automatically segmenting breast cancer in mammography images was presented. For breast mass segmentation, our method use a fully-automatic approach based on deep-learning technique. This technique combines attention gates (AGs) with densely linked U-Net for mammography segmentation. Additionally, the digital database for screening mammography (DDSM) database was used to test this strategy, and the results of the experiments revealed that dense U-Net coupled with AGs outperformed other approaches. The technique attained an overall accuracy of 78.38 percent, an F1 score of 82.24 percent, a sensitivity of 77.89 percent.

A deeply supervised U-Net was proposed by Ravitha et al., (2021) for bulk segmentation in digital mammograms (DS-U-Net). The DDSM and INbreast datasets were used in the evaluation of the approach, and cLare filter was used to boost the contrast in the photos. Whether the photos were preprocessed or not, the experiments were split into two groups. It was discovered that preprocessing had a positive impact on experiment results when compared to no preprocessing. Based on preprocessing, the technique achieved 99.70 percent in accuracy, 83.10 percent in sensitivity, and 99.80 percent in specificity. It also achieved a figure of 82.70 percent in Dice, and 85.70 percent in Jaccard coefficient.

When the work done in the area of joint segmentation and classification of mammography images was reviewed, it was discovered that Shen et al., (2020) proposed the mixed-supervision-guided, and residual-aided classification U-Net model (ResCU-Net). For noise reduction in the mammograms used, convolution filters were used. The MS-ResCU-Net model had 94.16% in accuracy, 93.11% in sensitivity, 95.02% in specificity, DI rates of 91.78 percent, Jaccard rates of 85.13 percent, and MCC (Mathew Correlation Coefficient), rates of 87.22%. While ResCU-Net had accuracy rates of 92.91 percent, Sensitivity of 91.51 percent, Specificity of 94.64 percent, DI of 90.50 percent, Jaccard of 83.02 percent, and MCC of 84.99 percent. Full-resolution Convolutional Network (FrCN), a new segmentation model for mammography images, was proposed in Al-antari et al., (2020).

Three conventional deep learning models were employed to categorize the identified, segmented lesions in breast as benign, or malignant. The models developed include CNN, ResNet-50, and InceptionResNet-V2. The INbreast database was accessed to

obtain mammography pictures. The performance metrics of these models for breast lesion segmentation that was based on FrCN was 92.97% for accuracy, 85.93% achieved for MCC, while 92.69% was achieved for Dice. The accuracy for Jaccard similarity index was 86.37%.

A deep learning and Conditional Generative Adversarial Networks (CGAN) model for breast density segmentation was proposed by Saffari et al., (2020). The segmentation of dense tissues that were present in mammograms images were segmented by using CGAN network. In order to carry out noise reduction, the images were subjected to median filtering before the performance was carried out. A total of 410 images from 115 patients retrieved from the INbreast dataset was used. Performance metrics revealed 98.0% for accuracy, Dice coefficient of 88.0% percent, and Jaccard similarity index of 78.0% were achieved. RCNN and DeepLab neural networks were used by Ahmed et al., (2020) to create semantic segmentation for cancer of the breast. The performance metrics were evaluated on two datasets, namely MIAS, and DDSM. Noise was eliminated using the edge-based Savitzky Golay filter. For RCNN the performance was 95.0% but for DeepLab, the method's AUC was 98.0%. However, the segmentation task's average precision was 80.0%.

H. Modified U-Net Segmentation

Hossain, (2022) presented micro calcification segmentation. The Laplacian filter was used to eliminate noise after training the suggested approach on images obtained from the DDSM database. Five steps made up the procedure: image preprocessing, segmentation of breast regions, extraction of suspicious patches, selection of positive patches, and training of the segmentation network. The technique resulted in a Dice score of 97.80 percent and an F-measure of 98.50 percent.

Additionally, it was found that the Jaccard index was 97.40 percent, and the proposed method's average accuracy was 98.20 percent. Tsochatzidis et al., (2021) presented a modified convolutional layer of a CNN model based on the U-Net model. DDSM-400, and Curated Breast Imaging Subset-Digital Database for Screening Mammography (CBIS-DDSM), were used as hybrid datasets for the method's evaluation.

The evaluation was based on the ground-truth segmentation maps. The approach obtained diagnostic performance metric of 89.8%, AUC value of 86.20%, and a value of 88.0% for DDSM-400, and a value of 86.0% for U-Net-based segmentation for CBIS-DDSM.

Based on the presented literature, models with attention have improved segmentation performance. However, the existing segmentation architectures have not fully addressed the issues of salient feature learning of mammograms to achieve state-of-the-art segmentation results. In this thesis work, a modified U-Net model based on increasing kernel sizes was presented, which leverages the squeeze and excitation attention mechanism with dimensionality reduction in its contrastive module. By doing this, an improved segmentation performance with low model complexity was achieved. The following section presents some general descriptions of convolutional, fully connected and pooling layers leveraged for biomedical image segmentation.

I. Machine Learning Algorithm

Machine learning (ML) algorithms processes and analyzes data in order to learn the underlying patterns about people, business operations, transactions, occurrences, etc. There are 4 types of ML algorithms, which are discussed in the following section.

1) Types of Machine Learning Algorithm

Machine Learning algorithms could be roughly divided into four groups: the supervised learning group, the unsupervised learning group, the semi-supervised learning group, and the reinforcement learning group.

a) Supervised machine learning Algorithms

In this group of machine learning, the machine learns how to map an input function into an output function based mainly on the supplied sample of the input-out pairs. This is done by making inference from a set of data supplied for training and another set supplied for testing. Learning becomes supervised if the goal to be achieved is given to the machine and a set of inputs are supplied as well. It is also known as task-driven approach to machine learning. Tasks that falls into this group include

classification tasks and regression tasks. They make predictions based on patterns learned from input data. Examples are tasks such as predicting a class label, or sentiment for a piece of text such as a tweet, or product review, using text classification.

b) Unsupervised machine learning

This is the process of analyzing data that are not labeled without human intervention. It is called a data driven approach to learning. This type of learning is commonly used to extract features that are generated from datasets, to find meaningful trends and patterns, to group data in results, and for the purpose of exploration. Popular among tasks that can be considered unsupervised tasks are clustering, learning of features, estimation of density, dimensionality reduction, finding association rules. The most popular Unsupervised Learning tasks are: clustering, density estimation, feature learning, dimensionality reduction, anomaly detection, computing association rules.

c) Semi-supervised machine learning

This is a hybrid of supervised learning and unsupervised learning because it works on both data that are labeled, and data that are not labeled. Semi supervised learning lies somewhere between supervised learning “unsupervised” and supervised learning “supervised”. In practice, data that are labeled may be sparse in many situations, while unlabeled data is abundant in many situations, where semi supervised learning can be useful.

d) Reinforcement Machine Learning

Reinforcement learning is a type of machine learning algorithm that can be used to train software agents, or machines, to be able to automatically assess the best behavior in a specific environment, or context, so as to improve its performance, which is based on an environment. This kind of learning is usually reward-based, or penalty-based. The goal of reinforcement learning is to be able to take action based on insights from environmental activities in order to increase reward, or minimize risk. Reinforcement Learning is a powerful AI model training tool, which can improve automation, or optimize the performance of complex systems like Robotics, Autonomous Driving, Manufacturing and Supply Chain Logistics, etc. However, it is not recommended to use reinforcement learning for the purpose of solving simple problems.

III. REVIEW OF RELATED WORKS

Zuluaga-Gomez, *et al.*, (2019) developed a CNN-based methodology for the diagnosis of breast cancer using thermal images. They proposed a CNN hyper-parameters, fine-tuning optimization algorithm, using a tree parzen estimator. The result achieved accuracy of 92%. However, the researchers used 57 breast cancer datasets, which is insufficient. Asri *et al.*, (2016) carried out the performance comparison of selected machine learning algorithms which include SVM, decision tree, KNN, and Naïve Bayes.

The Wisconsin Breast Cancer dataset was used in the experiment, which contains 699 instances of both malignant and benign cancer. Schaefer *et al.*, (2009) carried out a fuzzy logic based classification algorithm on 150 samples of breast cancer mammographic images. The performance evaluation carried out shows accuracy of 80%. This result was attributed to the use of statistical feature analysis, which is a key source of data for achieving such accuracy. The drawback of the research is mainly insufficient dataset used.

Sumathi *et al.*, (2007) proposed breast cancer diagnosis model that is based on genetic algorithm, and adaptive resonance theory neural network. The data used was sourced from Wisconsin Breast Cancer Data (WBCD). The data samples trained were 699 samples which were taken through Biopsy technique, also called the fine needle aspirates. The number of missing data were 16. Samples that contained breast tumours were 683 samples, which were used in this research. Sixty-five (65%) of the data were benign, and thirty-five (35%) were malignant. The developed model combined Probabilistic Neural Network (PNN) with Multilayer Perceptron (MLP) and the dataset used was sourced through Biopsy technique. This is very tedious when training the data. Adam and Omar, (2006) proposed a model for the detection of breast cancer. The work used a hybrid of genetic algorithm and Back Propagation Neural Network. This was done with the aim of reducing the detection time and increasing the detection accuracy. Different cleaning processes and data preprocessing were carried out on the dataset. The system recorded the detection accuracy of 83.36% Research in Mambou *et al.*, (2018) developed a breast cancer detection system using infrared thermal imaging

and deep learning. The model was trained using 67 images obtained through the dataset obtained from Research Data Base (DMR) containing frontal thermogram images that were acquired by the use of FLIR SC-620 IR camera, which has a resolution of 640×480 pixels. The testing of the model was carried out using 12 images that have breast cancer. Each image was augmented in order to generate additional 20 images each image. Performance evaluation of the model shows 88.5% in accuracy.

Khan *et al.*, (2019) presented a framework based on deep learning for the detection of cancer of the breast using transfer learning. Feature extraction was carried out and they used pretrained networks such as GoogLeNet, Visual Geometry Group Network (VGGNet), and Residual Networks (ResNet). The sample images were fed into a fully connected layer of the network. Classification into benign and malignant tumours were done using average pooling. Performance evaluation metric shows accuracy of 97.52%. in the preprocessing stage, 82 images were used, which were augmented to make a total of 8,000 images. Deep learning technique was used to extract features from raw images for classification process as stated in LeCun *et al.*,(2015). However, the concept of detection is general, and it does not entirely focus on segmenting the affected areas after detection. For this reason, researchers have adopted and proposed various segmentation models to segment tumours from breast cancer images.

IV. METHODOLOGY

The details of the algorithm, the system architecture, the description of the input, the preprocessing methods, and the feature extraction techniques are presented in this chapter. The design will help realize the overall objectives of this research. This research proposes adopting a modified U-Net model as the solution approach to achieve effective segmentation of tumours from breast cancer. The proposed system flow diagram of the whole method is presented in Figure 4.1.

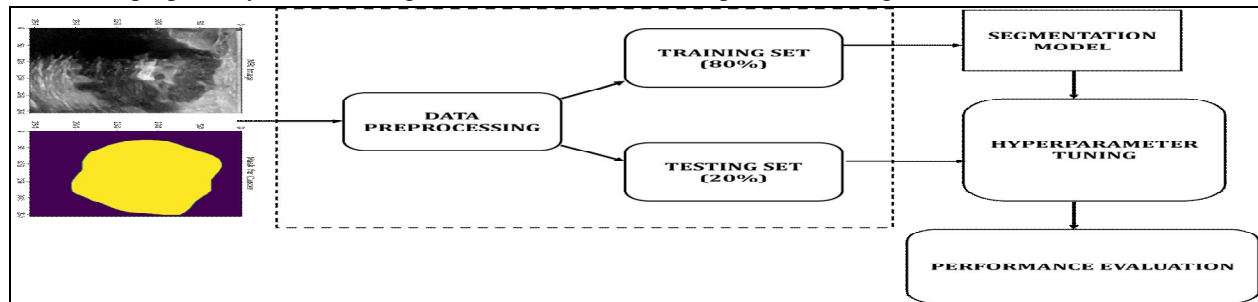


Figure 4. 1: Flow diagram of proposed Model

The images put into the system consist of MRI (Magnetic Resonance Imaging) image and the cancer image mask. These images enters the pre-processing stage where they are divided into training set and testing set.

A. Input Dataset

The dataset used for this research is the BUSI (Breast Ultrasound Images) dataset, publicly available with manually labelled ground truth. The dataset consists of 1312 images of various breasts diagnosed with benign and malignant cancers. The other class is the normal class, which we deleted in our method, as we focus on improving segmentation and not detection. Figure 4.2 shows the extract of the data.

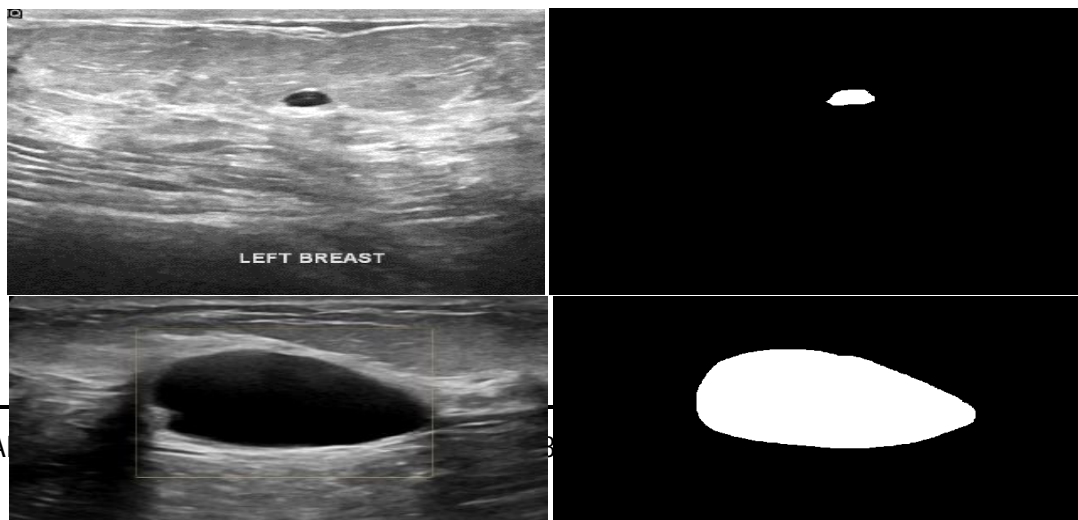


Figure 3.2 the extract of the data.

Figure 4.2 The extract of the data.

B. Data Normalization

The images in the dataset is in various sizes; however, we rescaled it to 256 x 256 before being fed to the segmentation model. The dataset was converted to an array using CV2.

C. Models

The models used in this research work for the purpose of achieving the objectives are presented in the following sub-sections.

1) U-Net Architecture

The U-Net architecture consist of the encoding and the decoding blocks, which uses Convolutional layers, batch normalization and max pooling layers in the encoder, and upsampling, convolutional transpose layers in the decoder. As shown in Figure 4.3, the U-Net architecture

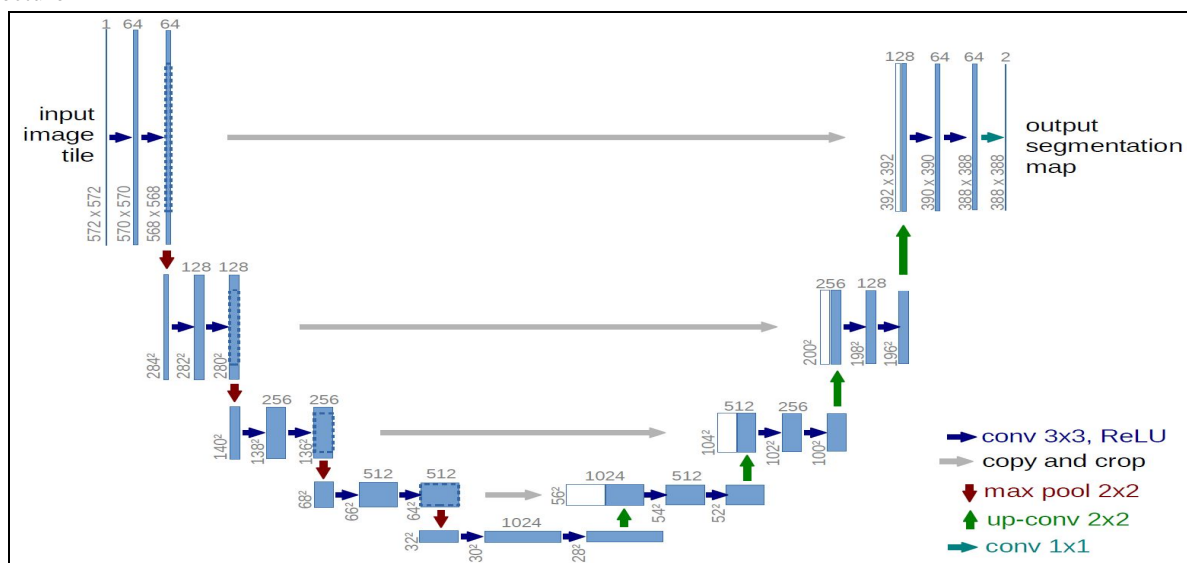


Figure 4. 3: General U-Net Architecture

In this research, we considered the U-Net as our benchmark model since our proposed model is based on modifying the benchmark. The figure shown in Figure 3.3 is the general U-Net architecture for a 572 x 572 image segmentation. However, our benchmark was implemented following the same configuration, but with 256 x 256 images. Also, the channel dimension of the benchmark U-Net starts from 16. This is well explained in the following section.

2) Baseline Model

In our baseline, we adopted progressively increasing kernel sizes rather than the fixed kernel sizes of the benchmark U-Net architecture, which uses convolutional blocks with 3x3 kernel sizes. By doing this, we can increase the feature learning ability of the U-Net architecture. The architecture of the baseline model is presented in Figure 4.4.

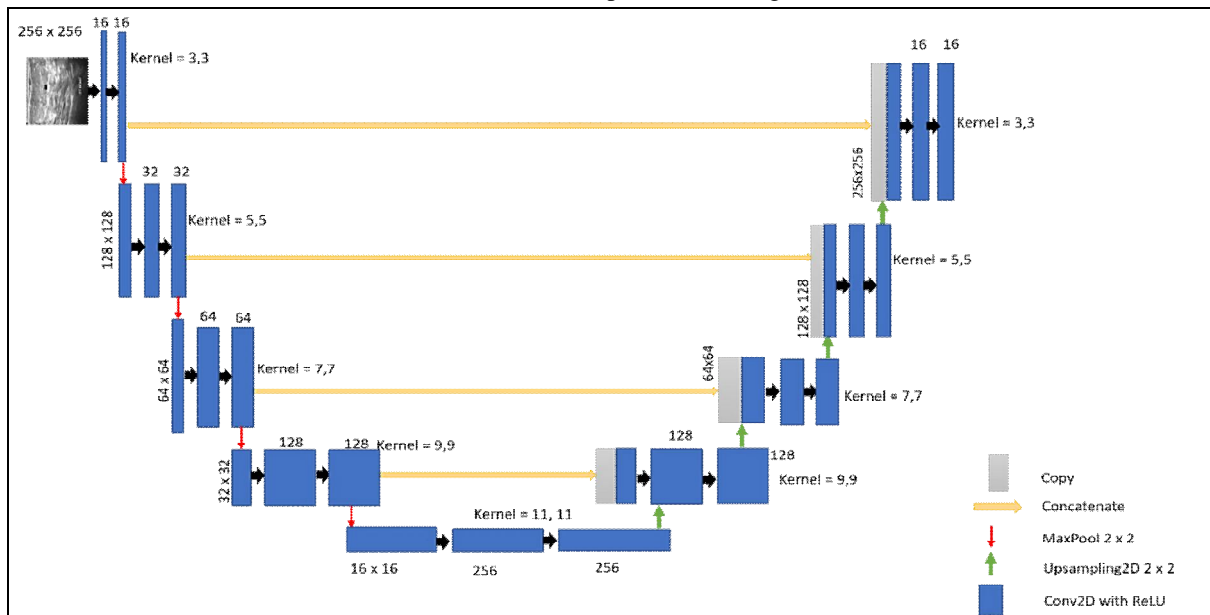


Figure 4. 4: Baseline model with increasing Kernel size

The kernel sizes 3x3, 5x5, 7x7, 9x9 and 11x11 was employed with channel dimension starting from 16 up to 256 in our baseline model. The only difference in our baseline model is the inclusion of the squeeze and excitation block.

3) Squeeze And Excitation Block

The squeeze and excitation block, first proposed in Hu *et al.*, (2018), uses two fully connected layers in a squeeze and exciting manner, where the first fully connected layer is reduced using a fixed reduction ratio. The architecture of the squeeze and excitation block is shown in Figure 4.5.

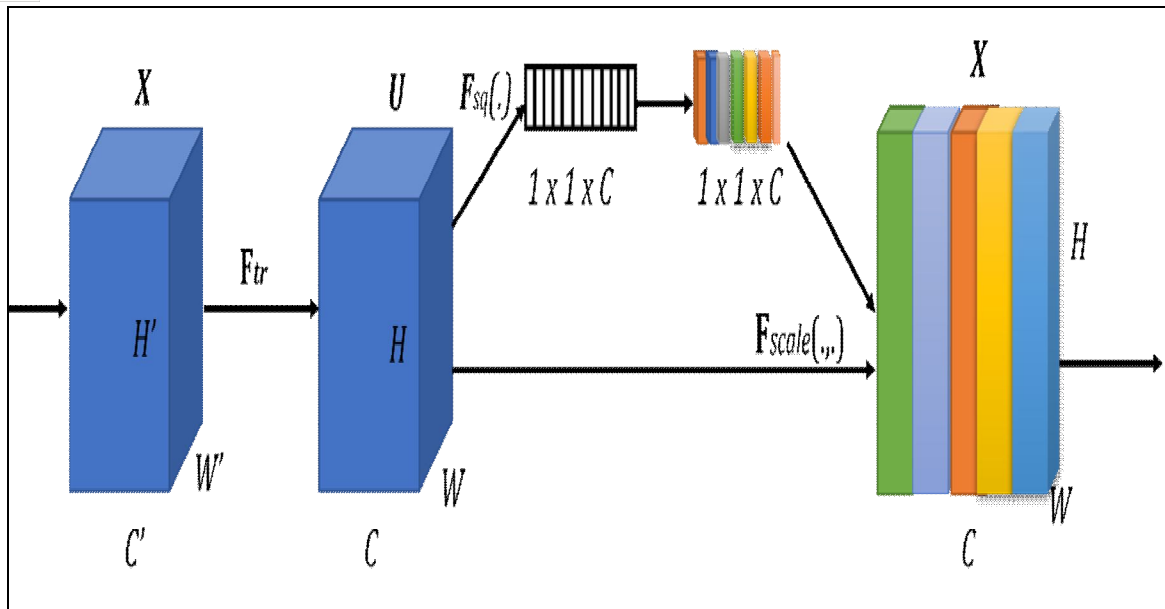


Figure 4. 5: Squeeze and Excitation Block

For any transformation, $F_{tr}: X \rightarrow U, X \in \mathbb{R}^{H' \times W' \times C'}$, $U \in \mathbb{R}^{H \times W \times C}$, eqn (1)

let $V = [v_1, v_2, \dots, v_c]$ denote the kernel filters, where v_c is the last kernel filter, the output of the transformation can therefore be given as:

$$U = [u_1, u_2, \dots, u_c]$$

Where

$$u_c = v_c * X = \sum_{s=1}^{C'} v_c^s * X^s \dots \dots \dots \text{eqn (2)}$$

* is the convolution operation, while v_c^s is the spatial kernel representing a single channel of v_c , which is the corresponding channel of X .

For dimensionality reduction, the first fully connected layer of the SE block used a ReLU (Rectified Linear Unit) activation function with the reduction ratio which is fixed at 8, which ensures that the features remain discriminative as it is being squeezed. Another fully connected layer which uses sigmoid activation function is then added to learn non-mutually exclusive relationship in the features, before rescaling with a multiply layer.

D. The Model

In the model, progressively increasing kernel sizes were used, which is different from the architecture of U-Net, which uses fixed 3x3 kernel size for all convolutional layers. The first Convolutional block having two Conv2D layers with 3x3 kernel sizes, ReLU (Rectified Linear Unit) activation function and 16 channel dimensions. A maxpooling2D layer with pool size of (2x2) was placed to downsample the image size before feeding to the next convolutional block which used the same activation function, with 32 channel dimension and 5x5 kernel size. The following convolutional block also used 64 channel dimensions with 7x7 kernel size, then a 9x9 kernel size Conv2D block with 128 channel dimensions was placed before the Conv2D with upsampling.

The squeeze and excitation block were placed after this convolutional layer and in-between the two convolutional blocks with 11x11 kernel sizes, to reallocate the weight of the essential features to ensure that more discriminate features are learnt from the

breast cancer images to improve segmentation performance. By using progressively increasing kernel sizes, the model can also learn more discriminate features. The architecture of the proposed model is shown in Figure 4.6.

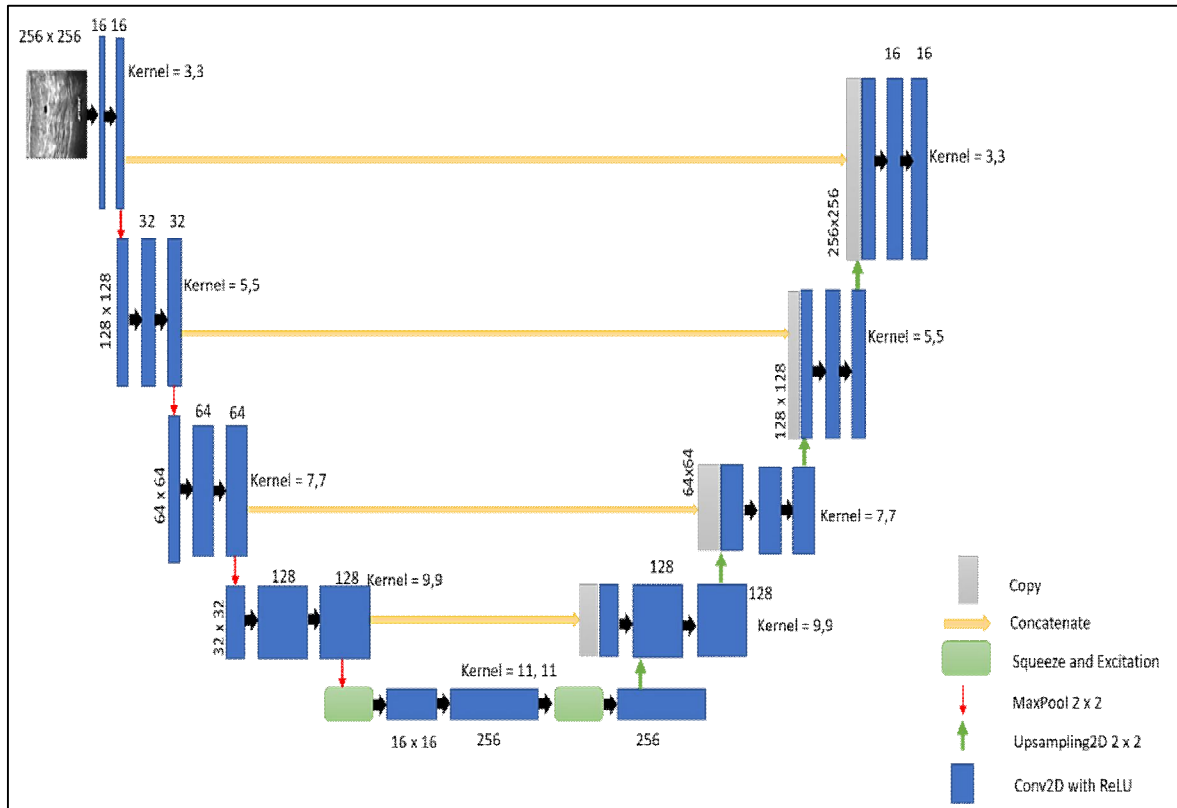


Figure 4 6: Architecture of the Proposed Model

E. Performance Evaluation

Performance evaluation is also known as performance appraisal or performance review. This is the process of assessing and measuring an individual's or a group's performance in relation to predetermine goals, objectives and standards. The purpose is to give a fee- back on a particular task performed. For the model evaluation, six standard metrics are used to compare the performance of the proposed ConvSegNet model to the existing methods. Jaccard, F1-Measure, Recall, Precision, Accuracy and F2-Measure were considered.

1) Jaccard similarity Index

$$\text{Jaccard Similarity Index} = \frac{S_{\text{Ground Truth}} \cap S_{\text{Automated}}}{S_{\text{Ground Truth}} \cup S_{\text{Automated}}} = \frac{TP}{TP+FP+FN} \quad \text{eqn (3)}$$

Jaccard similarity index is the difference between the overlap area between predicted and ground truth and the overlap area between the predicted segmentation and the ground truth segmentation (IoU). It is calculated as in equation (3), where S represents segmentation..

2) F1 Measure

$$F1_{\text{measure}} = 2 \times \frac{\text{Precision} \times \text{Recall}}{\text{Precision} + \text{Recall}} \quad \text{eqn (4)}$$

Equation (4) shows the formula for the difference between predicted and actual segmentation. F1 measure is also known as Dice Score. The F1 measure measures the difference between the predicted and the actual segmentation.

3) Precision

$$\text{Precision} = \frac{\text{Correctly Predicted tumours Pixel}}{\text{Total Number of Predicted tumours Pixels}} = \frac{TP}{TP+FP} \quad \text{eqn (5)}$$

Equation (5) shows that Precision refers to the difference between the number of predicted disease pixels and the total number of predicted ground truth pixels in biomedical segmentation.

Recall

$$\text{Recall} = \frac{\text{Correctly Predicted tumour Pixels}}{\text{Total Number of tumours pixels}} = \frac{TP}{Tp+FN} \quad \text{eqn (6)}$$

Equation (6) illustrates the formula to calculate recall. It takes into account the number of disease pixels per ground truth segment that the model segments correctly.

4) Accuracy

$$\text{Accuracy} = \frac{\text{Correctly Predicted Image Pixel}}{\text{Total number of Image Pixels}} = \frac{TP+TN}{TP+FP+FN+FP} \quad \text{eqn (7)}$$

As shown in equation (7), the model's accuracy considers the percentage of the image pixels that are correctly classified.

5) F2 measure

$$F2_{\text{measure}} = \frac{5 \times \text{Precision} \times \text{Recall}}{4 \times \text{Precision} + \text{Recall}} \quad (8)$$

The $F2_{\text{measure}}$ is more focused on the recall than precision, and it is suitable when it is more important to classify correctly as many positive samples as possible as shown in equation (8) above

V. IMPLEMENTATION AND TESTING

A. Hyperparameters

For hyperparameters tuning, we considered early stopping mechanism to halt the model once it stops improving. This was done by monitoring the validation loss of the model, with early stopping patience of 20. The remaining hyperparameters of the benchmark U-Net, the baseline U-Net and the proposed model are presented in Table 5.1.

Table 5.1: Hyperparameters Tuning

Hyper-parameters	Configuration
Epoch	100
Optimizer	Adam
Early stopping	Patience = 20
Reduce Learning rate	Patience = 10 Minimum LR = $1e^{-8}$ Maximum LR = $1e^{-4}$
Loss Function	Dice loss
Training Batch size	8
Kernel size in benchmark U-Net	3,3
Kernel Size in baseline U-Net and proposed model	3,3 – 5,5 – 7,7 – 9,9 – 11,11

SE reduction rate in proposed model	64
-------------------------------------	----

First the dataset was splitted into training set, and testing set. The percentage for training is 70%, the percentage for validation is 10%, while 20% was used for testing. For fair comparison, we applied the same hyperparameters shown in Table 4.1 to the model, except for the kernel sizes and the SE reduction rate, as those are the inclusions to be evaluated. Adam optimizer was used, with reduce learning rate function added to monitor the learning rate. Dice loss was then used as the loss function, with a batch size of 8.

B. Results

Following experiments, the model's performance on the benchmark U-Net, the baseline U-Net which we modified to have varying kernel sizes, and our proposed model which has increasing kernel sizes and the inclusion of the SE block, was recorded. A visual evaluation was carried out to show the difference in the performance of the models, and then evaluation was carried out based on the performance evaluation metrics that were suggested. Also, the evaluation of the complexity of the three models was done regarding their model size. This is shown in Figure 4.1.

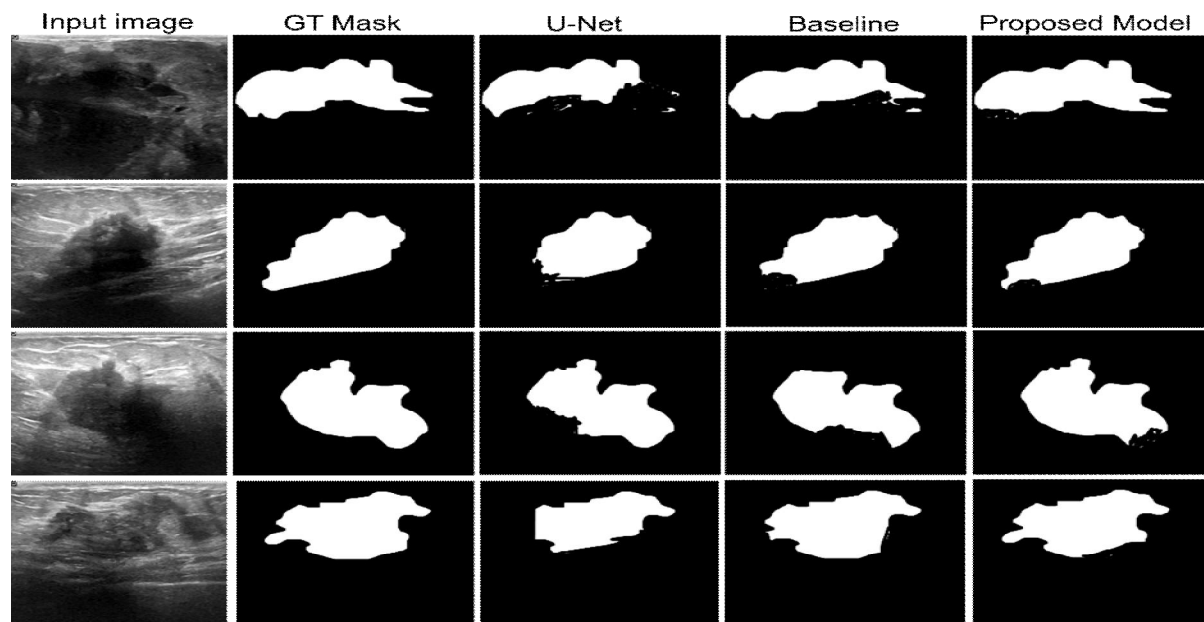


Figure 5. 1: Visualization Performance of the models

As shown in Figure 5.1, the input image and the ground truth mask were placed side by side, with the output of the three models stacked next. The U-Net had the most notable difference, which showed that the performance of the baseline model and the proposed model outperformed the U-Net. On close examination of the segmentation results of the baseline model, it is obvious that significant difference is visible in the masks segmented by the baseline model, which was reduced in our proposed model. For a state-of-the-art evaluation, the evaluation based on standard performance metrics is presented in Table 5.2

Table 5.2: Performance Evaluation of benchmark U-Net, baseline and the proposed Model

Model	Jaccard	F1	Recall	Precision	Accuracy	F2
U-Net	0.7743	0.7478	0.8983	0.7809	0.9648	0.8843
Baseline	0.8213	0.9120	0.9045	0.8745	0.9708	0.9136

Proposed Model	0.8750	0.9372	0.9318	0.9145	0.9881	0.9224
----------------	--------	--------	--------	--------	--------	--------

C. Model Benchmark

The performance evaluation result is presented in Table 4.2, the U-Net model achieved a Jaccard score of 0.7743, F1 of 0.7478, recall of 0.8983, precision of 0.7809, accuracy of 0.9648 and a F2 score of 0.8843.

The baseline model that used increasing kernel sizes, showed that a Jaccard score of 0.8213 was achieved, with a F1 of 0.9120, recall of 0.9045, precision of 0.8745, 0.9708 accuracy and a F2 score of 0.9136. However, the proposed segmentation model with an increased kernel size with two squeeze and excitation networks placed after the contraction block outperformed the benchmark and the baseline by achieving a Jaccard of 0.8750, F1 of 0.9372, recall of 0.9318, precision score of 0.9145, accuracy of 0.9881, and a F2 measure of 0.9224.

This result outperformed the benchmark with a difference of 0.1007 Jaccard score, 0.1894 F1 score, 0.0335 recall, 0.1336 precision score, 0.0233 accuracy, and 0.0381 F2 measure. Likewise the proposed model outperformed the baseline with a difference of 0.0537 Jaccard, 0.0252 F1, 0.0273 recall, 0.04 precision, 0.0233 accuracy and 0.0088 F2 measure. This result showed that our model achieved better segmentation performance than the benchmark U-Net and the baseline models

- 1) *Jaccard similarity index*: This similarity index is often used to detect how much similarity exist in sample sets. This can be defined as overlap length divided by the total union of the sample set under consideration. It emphasizes the resemblance that exist between finite sample sets. The visualization performance of Jaccard evaluation on models is represented by chart in Fig. 5.2.
- 2) *F1 score*:- This is used to evaluation classification models. It combines precision and recall into a single value, providing a balance measure of the developed model performance. The result of the evaluation is presented I the Fig 4.3 below

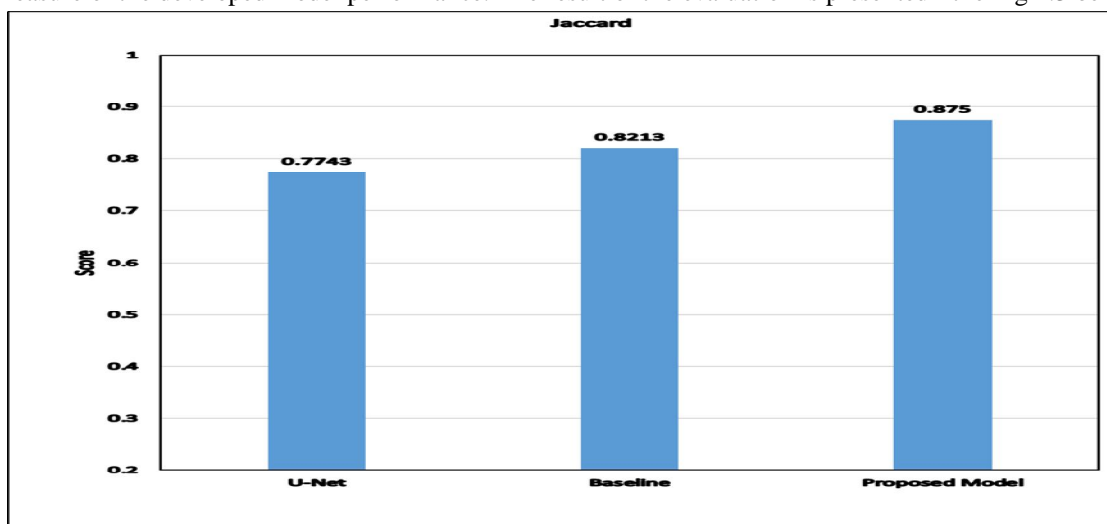


Figure 5. 2: Visualization Performance of Jaccard evaluation on models

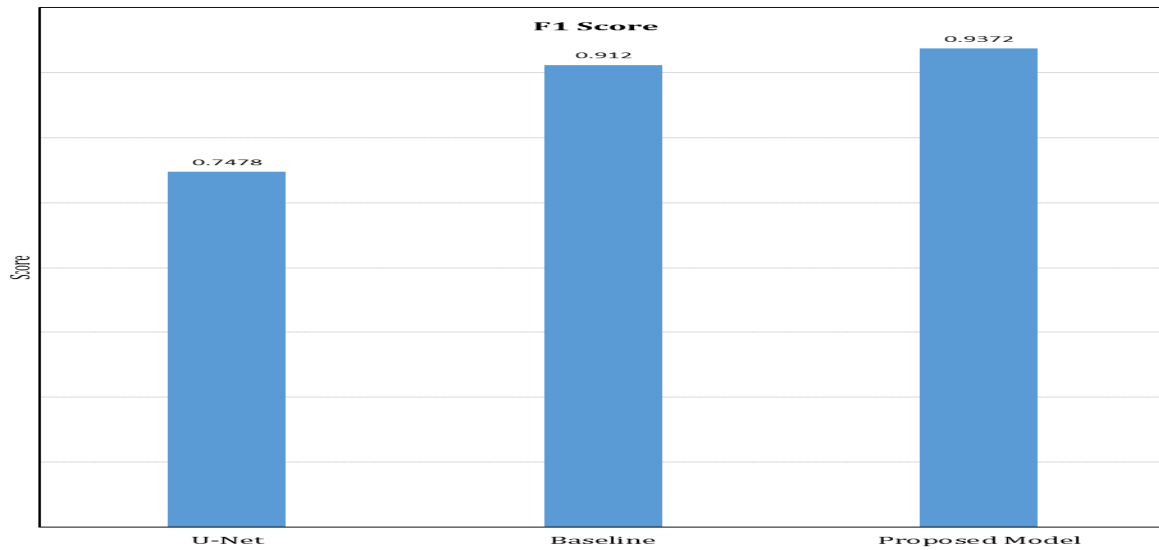


Figure 5. 3: Visualization Performance of F1 evaluation on models

- 3) *Recall*: This help in calculating the percentage of actual positives a model correctly identified (True Positive). When the cost of a false negative is high, you should use recall. The result from recall is represented in Fig 4.4 below

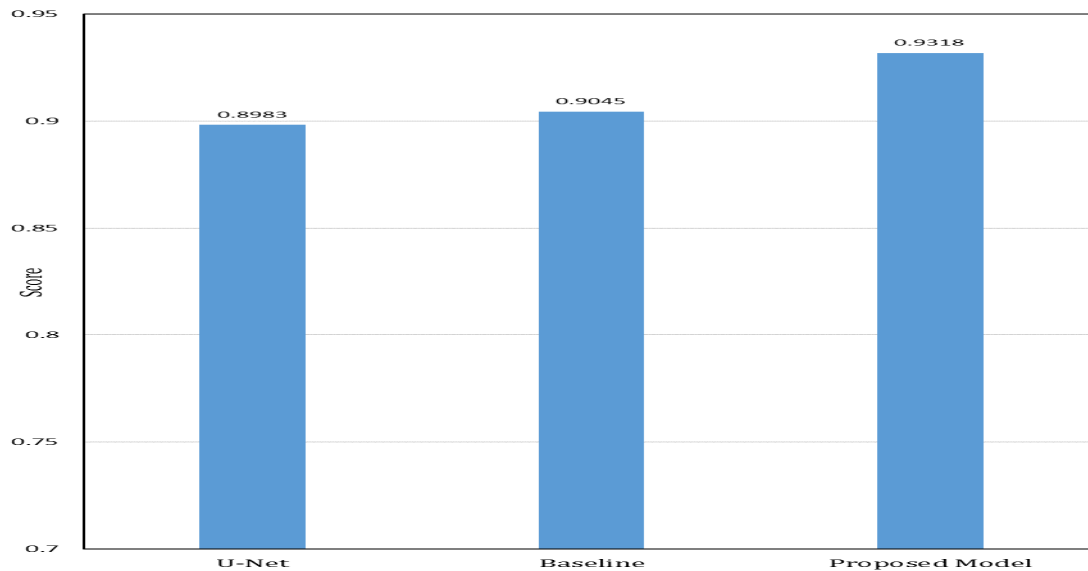


Figure 5. 4: Visualization Performance of Recall evaluation on models

- 4) *Precision*: This assesses how well the model predicts positive labels. Precision answers the question of how often the model was correct relative to how often it predicted positively Precision is the percentage of your results which are relevant and the result from our evaluation is presented in Fig 4.5 below

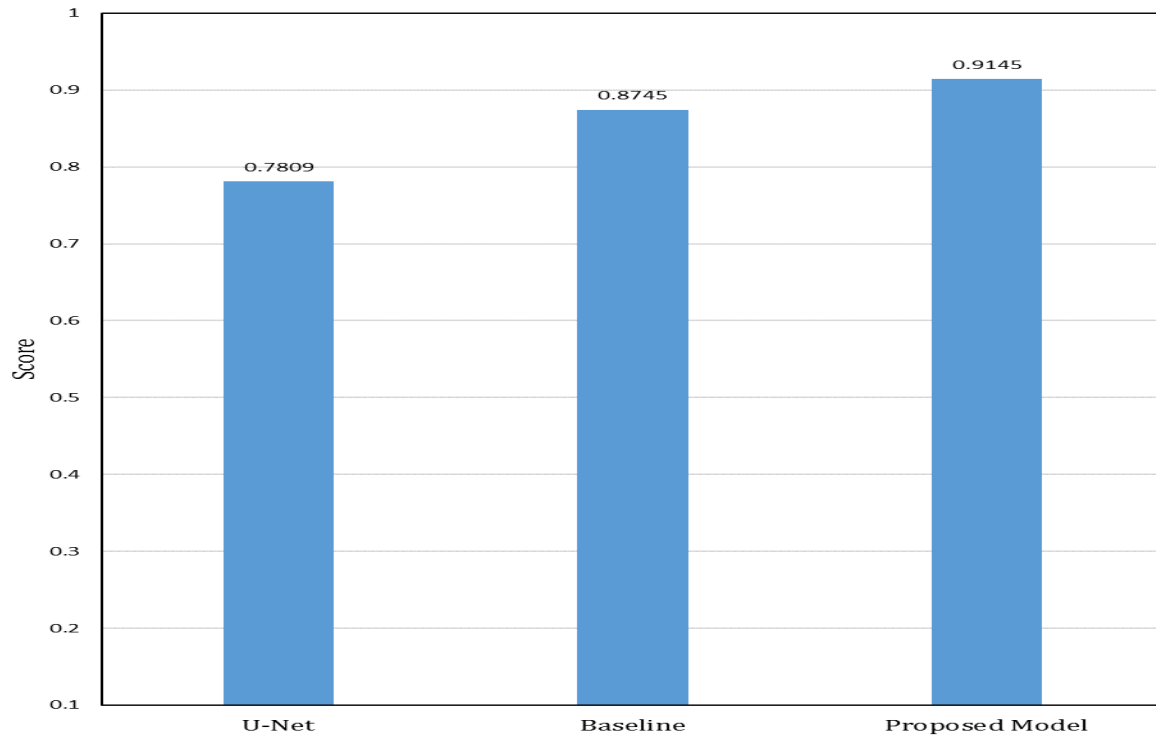


Figure 5.5: Visualization Performance of Precision evaluation on models

- 5) *Accuracy*: This is a metric that can be used to measure the total number of predictions that the model hits.. The result from the developed model is represented in Fig 5.6 below.

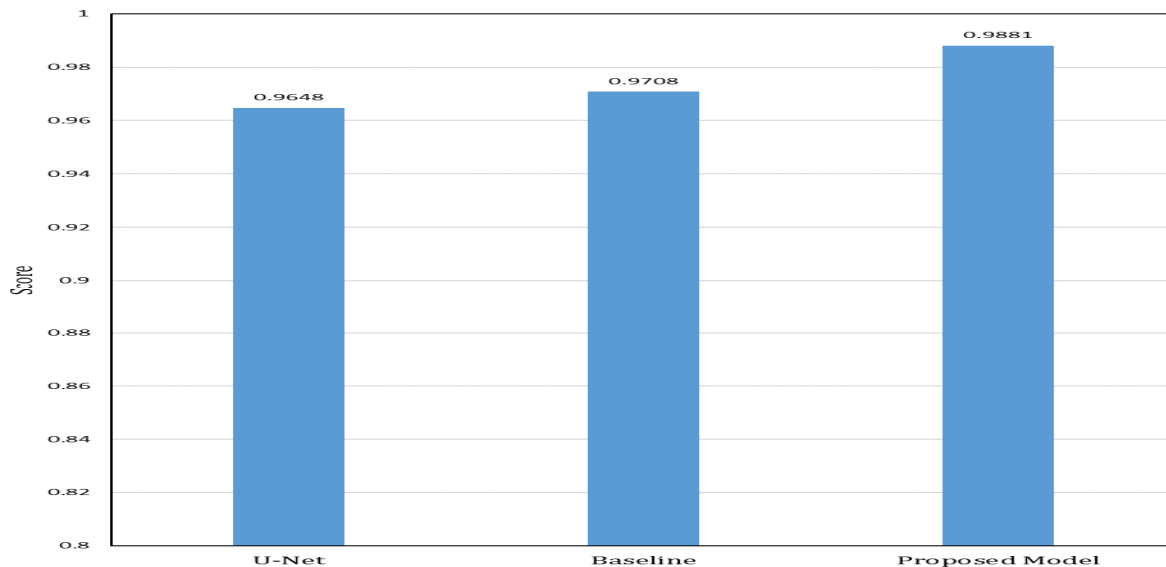


Figure 5.6: Visualization Performance of Accuracy evaluation on models

- 6) *F2 measure*:- This is used for classification models where recall is more important than accuracy. This is an extension of the F1 score and provides a method that focuses on accurately identifying positive cases. Similarity F1 and F2 scores combine precision and recall into one score. F2 puts more emphasis on memory by using different coefficients in the harmonic mean formula. The result gotten is presented in the Fig 5.7 below

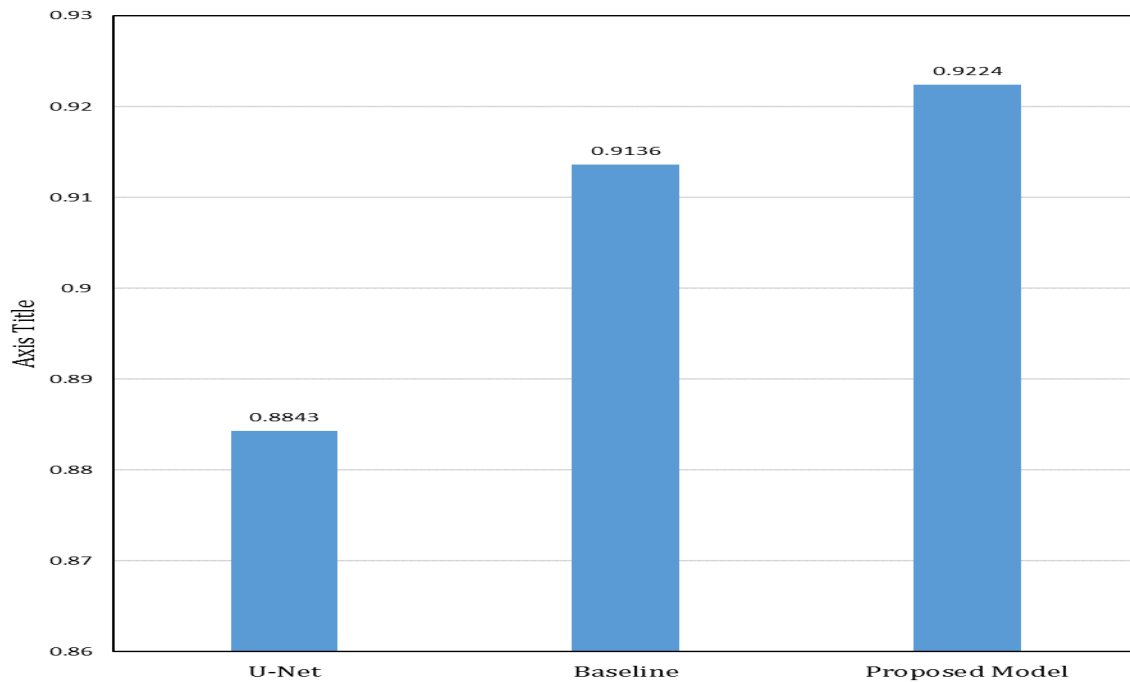


Figure 5. 7: Visualization Performance of F2 Measure evaluation on models

D. Model Complexity

As discussed earlier, the size of models is a major issue facing segmentation models. The model complexity with regards to the model size, presented in Table 4.3 shows that the U-Net architecture has 1.9M parameters, which is quite low, when compared to the baseline which has increasing kernel sizes. The baseline model has parameter value of 19.07M, which is quite large. However, by using the proposed model, a parameter value of 7.36M was achieved with higher segmentation performance.

Table 4.3 Size of Model Parameters

MODEL	TRAINABLE PARAMETERS	NON-TRAINABLE PARAMETERS
U-Net	1.9M	0
Our Baseline	19.07M	0
Proposed Model	7.36M	0

E. Discussion of Result

The experiments carried out in this research considered Jaccard, F1 score, recall, precision, accuracy and F2 measure as metrics. Also, we considered the model size for evaluation. As shown in Figure 4.1, the output of each segmentation model is visualized, and it can be seen that the segmentation obtained by the proposed model looks more similar to the ground truth mask. This was also validated, as shown in Table 4.2, where the performance of the proposed model outperformed the U-Net benchmark, and the baseline modified U-Net. This shows that by adding the squeeze and excitation block in our proposed model right after the contraction layer, more discriminant features were learnt.

The visualization of the metrics were presented in Figure 4.2 to Figure 4.7. Also, in Table 4.3, the model size of the three segmentation models were presented. The results showed that the proposed model had a 7.36 million parameters, which is high when compared to the benchmark U-Net. However, when compared to the baseline model which has 19.07 million parameters, the size of our proposed model is quite small, given that the proposed model outperformed the U-Net and the baseline U-Net, with few model complexity.



Several researchers have emphasized the importance of early and accurate breast cancer diagnosis, because it invariably reduces mortality rate. Early and accurate detection curbs issues arising from the metastatic nature of the ailment. Because of this, several researchers from various fields have proposed techniques to optimize the detection accuracy of breast cancer detection systems. The advent of Artificial Intelligence (AI) has motivated computer scientists to also contribute their quota into tackling the challenges.

Before accurate diagnosis can be done, segmentation of tumors from mammograms and ultrasound images of breast cancers is important. For this reason, various biomedical segmentation models have been proposed. However, challenges of low segmentation performance and bulky model size has been attributed to breast cancer segmentation images. To contribute to tackling this challenges, this research propose a novel biomedical segmentation model based on U-Net architecture. Progressively increasing kernel sizes were incorporated into the U-Net architecture, with two squeeze and excitation blocks placed at the last layer of the contraction block in our proposed model to act as channel attention with dimensionality reduction. By doing this, we were able to learn more discriminative features from the images and corresponding masks.

Results showed that our model outperformed the benchmark U-Net architecture which used a fixed 3x3 kernel size without the SE block and our baseline model which used progressively increasing kernel sizes without the SE blocks. The state-of-the-art segmentation performance achieved by our model came at a reduced model complexity, as a model size of 7.36M was recorded, against the 19.07M parameters of the baseline U-Net.

VI. CONCLUSION AND RECOMMENDATIONS

A. Conclusion

This research have proposed a novel segmentation model which uses channel attention with dimensionality reduction. In our model, we incorporated two squeeze and excitation blocks with the same configuration. Ablation studies were done to investigate the best reduction dimension in our model.

This enabled us to balance the tradeoff of model complexity and model performance. Likewise, we experimented by adding more SE blocks to the proposed model, and negligible increase was recorded in the segmentation performance, but it came at an increase complexity.

The proposed model in this research outperformed the baseline and the benchmark U-Net across all the considered performance evaluation metrics. Also, the size of our model is minimal, when compared to the baseline U-Net architecture.

B. Recommendation

The developed model is recommended for accurate segmentation of benign and malignant breast cancer tumours. The relatively small model size achieved in this research work make it suitable for deployment on mobile and embedded systems. This will make it readily available for use anywhere, anytime. Even though the segmentation model in this research was developed for breast cancer tumour segmentation, it can be easily trained and extended for other biomedical segmentation tasks such as segmentation of areas affected by tuberculosis in the lungs of human beings. It can also be deployed after training, for segmentation of brain tumours.

REFERENCES

- [1] Adam, A., & Omar, K. (2006). Computerized breast cancer diagnosis with Genetic Algorithm and Neural Network. Proc. of the 3rd International Conference on Artificial Intelligence and Engineering Technology (ICAIET), 22–24.
- [2] Ahmed, L., Iqbal, M. M., Aldabbas, H., Khalid, S., Saleem, Y., & Saeed, S. (2020). Images data practices for Semantic Segmentation of Breast Cancer using Deep Neural Network. Journal of Ambient Intelligence and Humanized Computing, 0123456789. <https://doi.org/10.1007/s12652-020-01680-1> AJCC. (2002). Breast. American Joint Committee on Cancer. Cancer Staging Manual, 223–240.
- [3] Al-antari, M. A., Al-masni, M. A., & Kim, T.-S. (2020). Deep Learning Computer-Aided Diagnosis for Breast Lesion in Digital Mammogram. In G. Lee & H. Fujita (Eds.), Deep Learning in Medical Image Analysis: Challenges and Applications (pp. 59–72). Springer International Publishing. https://doi.org/10.1007/978-3-030-33128-3_4
- [4] Asri, H., Mousannif, H., Al Moatassime, H., & Noel, T. (2016). Using Machine Learning Algorithms for Breast Cancer Risk Prediction and Diagnosis. Procedia Computer Science, 83(Fams), 1064–1069. <https://doi.org/10.1016/j.procs.2016.04.224>



- [5] Awad, A., Ali, A., & Gaber, T. (2020). Feature selection method based on chaotic maps and butterfly optimization algorithm. *Proceedings of the International Conference on Artificial Intelligence and Computer Vision (AICV2020)*, 1153, 159–169. <https://doi.org/10.1007/978-3-030-44289-7>
- [6] Boquete, L.; Ortega, S.; Miguel-Jimenez, J.M.; Rodriguez-Ascariz, J.M.; Blanco, R. (2012). Automated Detection of Breast Cancer in Thermal Infrared Images, Based on Independent Component Analysis. *J. Med. Syst.*, 36, 103–111.
- [7] Cardoso, F.; Harbeck, N.; Barrios, C.H.; Bergh, J.; Cortés, J.; El Saghir, N.; Francis, P.A.; Hudis, C.A.; Ohno, S.; Partridge, A. H. (2016). Research needs in breast cancer. *Ann. Oncol.*, 28, 208–217.
- [8] Carlson, R. W., Anderson, B. O., Chopra, R., Eniu, A. E., & Love, R. R. (2003). Treatment of breast cancer in countries with limited resources. *Breast J*, 9(2).
- [9] Chekkoury, A., Khurd, P., Ni, J., Bahlmann, C., Kamen, A., Patel, A., Grady, L., Singh, M., Groher, M., & Navab, N. (2012). Automated malignancy detection in breast histopathological images. *Medical Imaging 2012: Computer Aided Diagnosis*, 8315, International Society for Optics and Photonics.
- [10] Cruz-Roa, A., Gilmore, H., Basavanahally, A., Feldman, M., Ganesan, S., Shih, N. N. C., Tomaszewski, J., González, F. A., & Madabhushi, A. (2017). Accurate and reproducible invasive breast cancer detection in whole-slide images: A Deep Learning approach for quantifying tumor extent. *Scientific Reports*, 7(April), 1–14. <https://doi.org/10.1038/srep46450>
- [11] Dall, G., & Britt, K. (2017). Estrogen Effects on the Mammary Gland in Early and Late Life and Breast Cancer Risk. *Front Oncol*, 7, 110
- [12] Doersch, C. (2016). Tutorial on variational autoencoders. *ArXiv Preprint ArXiv:1606.05908*.
- [13] Eghbalian, S., & Ghassemian, H. (2018). Multi spectral image fusion by deep convolutional neural network and new spectral loss function. *International Journal of Remote Sensing*, 39(12), 3983–4002. <https://doi.org/10.1080/01431161.2018.1452074>
- [14] Fang, J., Zhou, Y., Yu, Y., & Du, S. (2017). Fine-Grained Vehicle Model Recognition Using A Coarse-to-Fine Convolutional Neural Network Architecture. *IEEE Transactions on Intelligent Transportation Systems*, 18(7), 1782–1792. <https://doi.org/10.1109/TITS.2016.262049>
- [15] Goodfellow, I. (2016). NIPS 2016 Tutorial: Generative Adversarial Networks. <http://arxiv.org/abs/1701.00160>
- [16] Horn, J., & Vatten, L. J. (2017). Reproductive and hormonal risk factors of breast cancer: a historical perspective. *International Journal of Women's Health*, 9, 265–272.
- [17] Hossain, M. S. (2022). Microcalcification Segmentation Using Modified U-net Segmentation Network from Mammogram Images. *Journal of King Saud University - Computer and Information Sciences*, 34(2), 86–94. <https://doi.org/https://doi.org/10.1016/j.jksuci.2019.10.014>
- [18] Hu, J., Shen, L., & Sun, G. (2018). Squeeze-and-Excitation Networks. *Proceedings of the IEEE Computer Society Conference on Computer Vision and Pattern Recognition*, 7132–7141. <https://doi.org/10.1109/CVPR.2018.00745>
- [19] Indolia, S., Goswami, A. K., Mishra, S. P., & Asopa, P. (2018). Conceptual Understanding of Convolutional Neural Network- A Deep Learning Approach. *Procedia Computer Science*, 132, 679–688. <https://doi.org/10.1016/j.procs.2018.05.069>
- [20] Irfan, R., Almazroi, A. A., Rauf, H. T., Damaševičius, R., Nasr, E. A., & Abdelgawad, A. E. (2021). Dilated semantic segmentation for breast ultrasonic lesion detection using parallel feature fusion. *Diagnostics*, 11(7), 1–20. <https://doi.org/10.3390/diagnostics11071212>
- [21] Khan, S. U., Islam, N., Jan, Z., Ud Din, I., & Rodrigues, J. J. P. C. (2019). A novel deep learning based framework for the detection and classification of breast cancer using transfer learning. *Pattern Recognition Letters*, 125, 1–6. <https://doi.org/10.1016/j.patrec.2019.03.022>
- [22] Khuriwal, N., & Mishra, N. (2018). Breast Cancer Detection from Histopathological Images Using Deep Learning. *3rd International Conference and Workshops on Recent Advances and Innovations in Engineering, ICRAIE 2018*, 2018(November), 1–4. <https://doi.org/10.1109/ICRAIE.2018.8710426>
- [23] LeCun, Y., Bengio, Y., & Hinton, G. (2015). Deep learning. *Nature* 521, 7553, 436.
- [24] Lee, H., Park, J., & Hwang, J. Y. (2020). Channel Attention Module with Multiscale Grid Average Pooling for Breast Cancer Segmentation in an Ultrasound Image. *IEEE Transactions on Ultrasonics, Ferroelectrics, and Frequency Control*, 67(7), 1344–1353. <https://doi.org/10.1109/TUFFC.2020.2972573>
- [25] Lee, K. B., Cheon, S., & Kim, C. O. (2017). A convolutional neural network for fault classification and diagnosis in semiconductor manufacturing processes. *IEEE Transactions on Semiconductor Manufacturing*, 30(2), 135–142. <https://doi.org/10.1109/TSM.2017.2676245>
- [26] Li, S., Dong, M., Du, G., & Mu, X. (2019). Attention Dense-U-Net for Automatic Breast Mass Segmentation in Digital Mammogram. *IEEE Access*, 7, 59037–59047. <https://doi.org/10.1109/ACCESS.2019.2914873>
- [27] Li, S., Johnson, J., Peck, A., & Xie, Q. (2017). Near infrared fluorescent imaging of brain tumor with IR780 dye incorporated phospholipid nanoparticles. *J. Transl. Med.*, 15.
- [28] Liu, X., Jiao, L., Tang, X., Sun, Q., & Zhang, D. (2019). Polarimetric Convolutional Network for PolSAR Image Classification. *IEEE Transactions on Geoscience and Remote Sensing*, 57(5), 3040–3054. <https://doi.org/10.1109/TGRS.2018.2879984>
- [29] Lynch, B., Neilson, H., & Friedenreich, C. (2011). Physical activity and breast cancer prevention. *Recent Results Cancer Res.*, 186, 13–42.
- [30] Mambou, S. J., Maresova, P., Krejcar, O., Selamat, A., & Kuca, K. (2018). Breast cancer detection using infrared thermal imaging and a deep learning model. *Sensors (Switzerland)*, 18(9). <https://doi.org/10.3390/s18092799>
- [31] Michael, E., Ma, H., Li, H., Kulwa, F., & Li, J. (2021). Breast Cancer Segmentation Methods: Current Status and Future Potentials. *BioMed Research International*, 2021. <https://doi.org/10.1155/2021/9962109>
- [32] Moody, S. E., Perez, D., Pan, T. C., Sarkisian, C. J., Portocarrero, C. P., Sterner, C. J., Notorfrancesco, K. L., Cardiff, R. D., & Chodosh, L. A. (2005). The transcriptional repressor snail promotes mammary tumor recurrence. *Cancer Cell* 8, 3 (2005), 197–209. *Cancer Cell*, 8(3), 197–209.
- [33] NBCF. (2016). National Breast Cancer Foundation. Breast Cancer Facts; National Breast Cancer Foundation: Sydney, Australia.
- [34] Rampun, A., Scotney, B. W., Morrow, P. J., & Wang, H. (2018). Breast Density Classification Using Local Quinary Patterns with Various Neighbourhood Topologies. *J. Imaging*, 4, 14.
- [35] Ravitha Rajalakshmi, N., Vidhyapriya, R., Elango, N., & Ramesh, N. (2021). Deeply supervised u-net for mass segmentation in digital mammograms. *International Journal of Imaging Systems and Technology*, 31(1), 59–71.
- [36] Ronneberger, O., Fischer, P., & Brox, T. (2015). U-net: Convolutional networks for biomedical image segmentation. *Lecture Notes in Computer Science (Including Subseries Lecture Notes in Artificial Intelligence and Lecture Notes in Bioinformatics)*, 9351(Cvd), 234–241. https://doi.org/10.1007/978-3-319-24574-4_28
- [37] Rouhi, R., Jafari, M., Kasaei, S., & Keshavarzian, P. (2015). Benign and malignant breast tumors classification based on region growing and CNN segmentation. *Expert Systems with Applications*, 42(3), 990–1002. <https://doi.org/10.1016/j.eswa.2014.09.020>
- [38] Saffari, N., Rashwan, H. A., Abdel-Nasser, M., Kumar Singh, V., Arenas, M., Mangina, E., Herrera, B., & Puig, D. (2020). Fully Automated Breast Density



- Segmentation and Classification Using Deep Learning. *Diagnostics*, 10(11). <https://doi.org/10.3390/diagnostics10110988>
- [39] Schaefer, G., Závisek, M., & Nakashim, T. (2009). Thermography based breast cancer analysis using statistical features and fuzzy classification. *Pattern Recognition*, 42(6), 1133–1137.
- [40] Shen, T., Gou, C., Wang, J., & Wang, F.-Y. (2020). Simultaneous Segmentation and Classification of Mass Region From Mammograms Using a Mixed-Supervision Guided Deep Model. *IEEE Signal Processing Letters*, 27, 196–200. <https://doi.org/10.1109/LSP.2019.2963151>
- [41] Siegel, R., Miller, K., & Jemal, A. (2017). Cancer Statistics. *CA Cancer J Clin*, 67, 7–30.
- [42] Smith, R. A., Cokkinides, V., & Eyre, H. J. (2003). American Cancer Society guidelines for the early detection of cancer. *CA Cancer J Clin*, 53, 27–43.
- [43] Spanhol, F. A., Oliveira, L. S., Petitjean, C., & Heutte, L. (2016). A Dataset for Breast Cancer Histopathological Image Classification. In *IEEE Transactions on Biomedical Engineering*, 7, 1455–1462. <https://doi.org/doi:10.1109/TBME.2015.2496264>.
- [44] Stewart, B. ., & Wild, C. P. (2014). *World Cancer Report 2014*. WHO Press.
- [45] Sumathi, C. P., Santhanam, T., & Punitha, A. (2007). Combination of genetic algorithm and ART neural network for breast cancer diagnosis. *Asian Journal of Information Technology*, Medwell Journals.
- [46] Sun, Y. S., Zhao, Z., Yang, Z. N., Xu, F., Lu, H. J., Zhu, Z. Y., Shi, W., Jiang, J., Yao, P. P., & Zhu, H. P. (2017). Risk factors and preventions of breast cancer. *International Journal of Biological Sciences*, 13(11), 1387–1397. <https://doi.org/10.7150/ijbs.21635>
- [47] Tsochatzidis, L., Koutla, P., Costaridou, L., & Pratikakis, I. (2021). Integrating segmentation information into CNN for breast cancer diagnosis of mammographic masses. *Computer Methods and Programs in Biomedicine*, 200, 105913. <https://doi.org/https://doi.org/10.1016/j.cmpb.2020.105913>
- [48] Usha, R. (2010). Parallel Approach for Diagnosis of Breast Cancer using Neural Network Technique. *International Journal of Computer Applications*, 10(3).
- [49] Vargas, H. I., Anderson, B. O., Chopra, R., Lehman, C. D., Ibarra, J. A., Masood, S., & Vass, L. (2003). Diagnosis of breast cancer in countries with limited resources. *Breast Journal*, 9(SUPPL. 2). <https://doi.org/10.1046/j.1524-4741.9.s2.5.x>
- [50] WHO. (2014). WHO Position paper on mammography screening, World Health Organization.
- [51] Wikipedia. (2020). Residual Neural Network <http://en.m.wikipedia.org>
- [52] Yang, J., Zhu, J., Wang, H., & Yang, X. (2021). Dilated MultiResUNet: Dilated multi-residual blocks network based on U-Net for biomedical image segmentation. *Biomedical Signal Processing and Control*, 68(April), 102643. <https://doi.org/10.1016/j.bspc.2021.102643>
- [53] Zheng, J., Lin, D., Gao, Z., Wang, S., He, M., & Fan, J. (2020). Deep Learning Assisted Efficient AdaBoost Algorithm for Breast Cancer Detection and Early Diagnosis. *IEEE Access*, 8, 96946–96954. <https://doi.org/10.1109/ACCESS.2020.2993536>
- [54] Zhou, Z., Rahman Siddiquee, M. M., Tajbakhsh, N., & Liang, J. (2018). Unet++: A nested u-net architecture for medical image segmentation. *Lecture Notes in Computer Science (Including Subseries Lecture Notes in Artificial Intelligence and Lecture Notes in Bioinformatics)*, 11045 LNCS, 3–11. https://doi.org/10.1007/978-3-030-00889-5_1
- [55] Zhu, W., Xiang, X., Tran, T. D., Hager, G. D., & Xie, X. (2018). Adversarial deep structured nets for mass segmentation from mammograms. 2018 IEEE 15th International Symposium on Biomedical Imaging (ISBI 2018), 847–850. <https://doi.org/10.1109/ISBI.2018.8363704>
- [56] Zuluaga-Gomez, J., Al Masry, Z., Benaggoune, K., Meraghni, S., & Zerhouni, N. (2021). A CNN-based methodology for breast cancer diagnosis using thermal images. *Computer Methods in Biomechanics and Biomedical Engineering: Imaging and Visualization*, 9(2), 131–145. <https://doi.org/10.1080/21681163.2020.1824685> *Journal of Innovative Research in Computer and Communication Engineering*, 4, 15772–15775.



10.22214/IJRASET



45.98



IMPACT FACTOR:
7.129



IMPACT FACTOR:
7.429



INTERNATIONAL JOURNAL FOR RESEARCH

IN APPLIED SCIENCE & ENGINEERING TECHNOLOGY

Call : 08813907089  (24*7 Support on Whatsapp)